# EMBEDDED HARDWARE AND SOFTWARE

# DESIGN FOR

# LOW-POWER WIRELESS ECG DEVICE

DAVID WONG LIANG TAI

NATIONAL UNIVERSITY OF SINGAPORE

2014

# EMBEDDED HARDWARE AND SOFTWARE

# DESIGN FOR

# LOW-POWER WIRELESS ECG DEVICE

## DAVID WONG LIANG TAI

*(B.Eng. (Hons.), Curtin University of Technology,*

*Australia)*

A THESIS SUBMITTED

FOR THE DEGREE OF MASTER OF ENGINEERING

DEPARTMENT OF ELECTRICAL

AND COMPUTER ENGINEERING

NATIONAL UNIVERSITY OF SINGAPORE

2014

# DECLARATION

I hereby declare that the thesis is my original work and it has been written by me in its entirely. I have duly acknowledged all the sources of information which have been used in the thesis.

This thesis has also not been submitted for any degree in any university previously.

_____

David Wong Liang Tai

25$^{th}$ March 2014

# ACKNOWLEDGEMENTS

# TABLE OF CONTENTS

# SUMMARY

As personalized healthcare devices come into mainstream of lifestyle gadgets, system engineers are challenged to design miniaturized devices that are power-aware, comfortable and intuitive to use. Arising from these challenges, this thesis focuses on the system level power optimization aspects of a Classic Bluetooth ECG (CB ECG) device and a Bluetooth Low Energy ECG (BLE ECG) device during continuous transmission.

The high level requirements for the wireless ECG device are described and translated into the Unified Modeling Language (UML) diagrams. The requirements include the need for the ECG device to stream continuous ECG data to a portable gateway (smartphone). These requirements are carefully studied and captured. The hardware components are listed and the firmware design is modeled by the UML diagrams such as the sequence diagram for component interaction, state machine diagrams for overall firmware behavioral design, etc. It should be noted that Bluetooth technology is chosen as the preferred wireless communication interface between the ECG device and the smartphone because it is widely adopted by smartphone manufacturers.

The main components in the CB ECG device are an analogue front-end ECG sensor, on-device flash storage, a microcontroller and a Classic Bluetooth transceiver module. The hardware of the CB ECG device is pre-designed. The frequency scaling technique is applied onto the microcontroller

and the flash storage is toggled between active and standby mode to reduce power. The overall power consumption falls to around 102.3mW. However, through system-level power profiling, it is found that more than 95% of the power consumption is dissipated by the microcontroller and the Classic Bluetooth transceiver module.

A ground-up investigation on hardware and software design was carried out and an integrated system-on-a-chip (SoC) containing a microcontroller and Bluetooth Low Energy transceiver was chosen for the Bluetooth Low Energy ECG (BLE ECG) device. The average current consumption drops to about by 6mA, owing to the integrated SoC. In addition, further power reduction is observed when a low-complexity lossless compression algorithm is implemented on the SoC. The average current consumption during transmission has been recorded to a mere 5mA (16.5mW) enabling at least 3 days of continuous real-time monitoring on a 420mAh battery. The BLE ECG device is also supported by a power management chip which reduces the dynamic power and static power dissipation via lower voltage supply and power gating alike mechanisms respectively. A system-level battery discharge plot against operational time is drawn for comparison against prior designs.

# LIST OF TABLES

# LIST OF FIGURES

# LIST OF ABBREVIATIONS

ADC – Analog to Digital Converter

AFE – Analog Front-End

BLE – Bluetooth Low Energy

BLE ECG – Bluetooth Low Energy ECG

CB ECG – Classic Bluetooth ECG

CMOS – Complementary Metal-Oxide Semiconductor

CPU – Central Processing Unit

CRC – Cyclic Redundancy Check

ECG – Electrocardiogram

FEC – Forward Error Correction

GUI – Graphical User Interface

Hz – Hertz

IC – Integrated Circuit

$I^2C$ – Inter-Integrated Circuit

I/O – Input/Output

ISM – Industrial, Scientific and Medical

IEEE - Institute of Electrical and Electronics Engineers

JTAG – Joint Test Action Group

LED – Light Emitting Diode

MCU – Microcontroller Unit

MIT-BIH – Massachusetts Institute of Technology - Beth Israel Hospital

NUS – National University of Singapore

PCB – Printed Circuit Board

PMIC – Power Management Integrated Circuit

SoC – System-on-Chip

SPI – Serial Peripheral Interface

SPS – Samples Per Second

UART – Universal Asynchronous Receiver/Transmitter

UML – Unified Modeling Language

# 1  INTRODUCTION

## 1.1  Motivation of the Work

Advancements in personal telemetry medical systems in recent years have become the recipe to meet the healthcare demands. The demand is mainly stirred by aging population requiring more quality attention. In addition to improving the quality of life, the prevention-oriented model and pervasive monitoring is generally preferred as prevention and early detection of diseases increase the chances of complete recovery. In addition, this technique requires medical professionals to have the patient's current and past medical records.

In the US, 3.6% of the population are affected by some kind of heart rhythm disorder [1]. Based on current trends, the most common heart rhythm disorders, arrhythmia and atrial fibrillation, is expected to double in the next 30 years [2]. Given the need to improve the point of care for patients suffering from chronic diseases, suspected patients are usually prescribed with an electrocardiogram (ECG) for a non-invasive and risk-free diagnosis. In 2009, it was recorded that the US has spent more than $3.47 billion on 68 million ECG tests. The amount is expected to soar by 9% in another 3 years. Early detection for patients suffering from atrial fibrillation enables cardiologist to prevent further complications and to advise on the treatment path. However, arrhythmia events are sporadic. This situation ignites the need for ECG devices that can support long-term monitoring which are wearable for better patient care [3].

From the patients' perspective, the wired-based ECG monitoring devices, such as Holter, are considered to be bulky, obtrusive (wire clutter on the chest) and uncomfortable. Such devices compromise the comfort and lifestyle resulting to low acceptance rate among patients. Recently, wireless ECG devices are introduced to reduce the wire clutter of the Holter. The ability to have continuous wireless ECG monitoring comes at a cost of higher power dissipation. The higher power requirement on a limited battery capacity hinders the ability to perform long-term wireless ECG monitoring.

A straightforward solution is to embed a larger battery capacity. However, a larger battery capacity is heavier and a larger-size battery compromises the patient's comfort when worn. Another less subtle solution is to rely on the latest battery technology. However, the improvement in battery storage densities (Watt-hour per kilogram, Wh/kg) is very slow. The Nickel-Cadmium (NiCd) technology, invented in 1899, has only showed a mere improvement of 3 folds when compared to the latest Li-Ion batteries [4].

Given the setback in battery density and the need to deliver better power performance for the wireless ECG device, several embedded low-power technologies and techniques can be applied to reduce power consumptions. In this thesis, two wireless ECG devices will be introduced, the Classic Bluetooth ECG (CB ECG) device and the Bluetooth Low Energy ECG (BLE ECG) device. The hardware of the CB ECG device is pre-designed [5] and the firmware is designed and implemented to reduce power dissipation [6]. The

hardware and software of the BLE ECG device is designed from ground-up to allow more power savings.

## 1.2    Contributions and Publications

The CB ECG device is developed using a discrete microcontroller (MCU) and Classic Bluetooth module. It initially consumes about 42mA during continuous transmission with voltage supply held at around 3.3V. The current consumed by the CB ECG device is reduced to about 31.5mA after applying the frequency scaling technique on the MCU and introducing active/idle switching technique on the local flash. The occasional use of the transceiver (31.5mA) and on-device recording (0.45mA) enables continuous operation of at least 1 month on a typical Li-Ion battery of 420mAH.

The low-power BLE ECG device is designed and implemented on an integrated system-on-a-chip (SoC) which consists of an MCU and a Bluetooth Low Energy (BLE) transceiver. The ECG device leverages on the integration of components into a single SoC to improve power consumption as compared to the decoupled MCU and transceiver module used by the multi-lead ECG device. The lossless gradient-based compression technique is also implemented onto the SoC's MCU to reduce the usage of the BLE transceiver for further power improvements. After the implementation of the compression technique, the current drawn from the device is reduced from 6.18mA to 5.06mA enabling at least 3 days of continuous real-time monitoring on a 420mAh Li-Ion battery.

The following items on the list are the publications generated from this project.

[1]    D. L. T. Wong and Y. Lian, "A wearable wireless ECG sensor with real-time QRS detection for continuous cardiac monitoring," *IEEE Biomedical Circuits and Systems Conference (BioCAS)*, 2012, pp. 112–115.

[2]    C. J. Deepu, X. Zhang, W.-S. Liew, D. L. T. Wong, and Y. Lian, "An ECG-SoC with 535nW/Channel Lossless Data Compression for Wearable Sensors," *IEEE Asian Solid-State Circuits Conference (A-SSCC)*, 2013, pp. 145–148.

[3]    C. J. Deepu, X. Zhang, W.-S. Liew, D. L. T. Wong, and Y. Lian, "An ECG-SoC with 535nW/Channel Integrated Lossless Data Compressor for Wearable Sensors," *IEEE Journal of Solid-State Circuits (JSSC)*, submitted in Jan 2014.

[4]    X. Zhang, C. J. Deepu, W.-S. Liew, D. L. T. Wong, X. Xu, and Y. Lian, "A 13.4 µA ECG and Respiration Acquisition SoC for Wearable Sensor Applications," *IEEE Transactions on Biomedical Circuits and Systems (TB-CAS)*, under preparation.

## 1.3    Thesis Organizations

The outline of the thesis is divided into seven main sections as listed below:

❖ Section 2: Overview of Wireless ECG System – An overview of the ECG
and the theoretical aspects of the inner workings of a wireless ECG device.
This section includes the comparison against existing solutions which
leads to the formulation of the features in the ECG device and its power
targets.

❖ Section 3: Principles of Low-Power Embedded Design – Describes the
general power optimization techniques for embedded devices. The
selection of wireless transceiver standard between Wi-Fi, ZigBee and
Bluetooth will be discussed. This is followed by general overview for the
need of compression prior to transmission.

❖ Section 4: Hardware Platform for Wireless ECG Device – The hardware
components needed to create a wireless ECG device.

❖ Section 5: Unified Software Platform for ECG System – The firmware and
application software design of a wireless ECG device and client
application.

❖ Section 6: Power Optimization Using Co-Design Techniques – The power
optimization techniques applied onto the CB ECG device and BLE ECG
device. It also contains the battery discharge plot. The validation and
verification process using a checklist was carried out to ensure that the
features and power-requirements are met.

❖ Section 7: Conclusion and Future Works – Concluding remarks about the
thesis.

# 2 Overview of Wireless ECG System

## 2.1 ECG Overview

Electrocardiography (ECG) is a technique to capture the electrical activities of a heart against time. The heart is an organ that pumps blood throughout the body in a rhythmic fashion called a heartbeat. Electrical impulses captured in an ECG test provide rich information about the biological activities of the heart, which helps medical professionals to identify heart problems. ECG is usually the preferred choice for diagnosis because it is non-intrusive and painless. In addition, it has been carefully studied over the years and has been accepted even as a predictor for cardiac and non-cardiac related diseases [7] [8].

Early studies in the 1950s and 1970s have shown that the ECG signal is generated from the depolarization and repolarization processes in the heart cell generating a propagation of dipole wavefronts across the tissue of the heart. Figure 1 illustrates a single cycle regular Lead II ECG signal drawn on a standard ECG paper. The major deflections are labeled in alphabetical order, namely, P wave, QRS complex, T wave and U wave [9].

The P wave is relative to the atrial depolarization. Following that, the QRS complex corresponds to the ventricular depolarization. Note that the atria repolarization also occurs during the QRS complex but its amplitude is insignificant in the ECG waveform. The T wave refers to the repolarization of the ventricles.
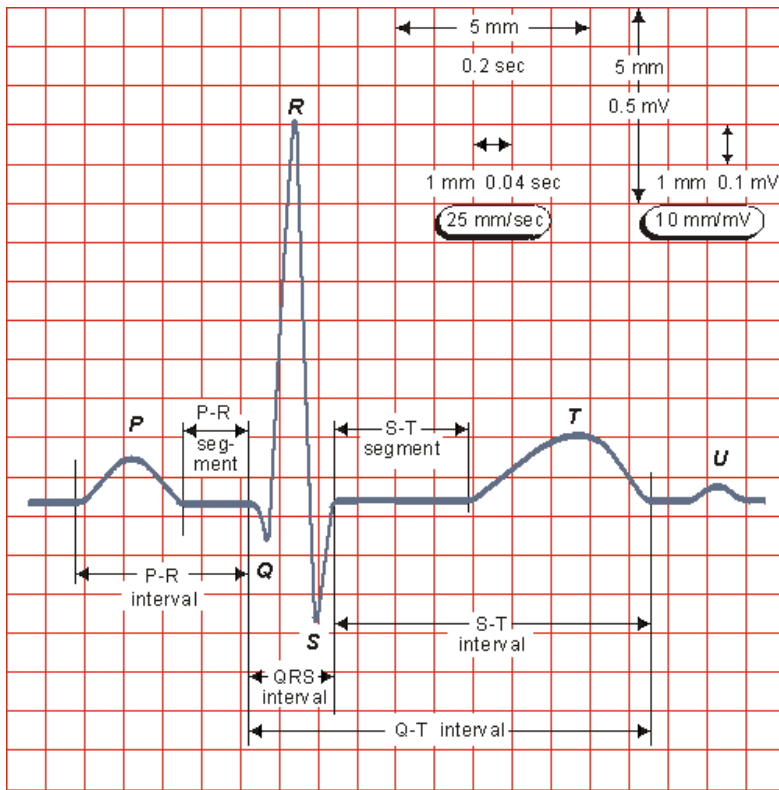
**Figure 1: The regular ECG signal in one cardiac cycle** [9]

These waves and segments are measured and commonly used by medical professionals for diagnosis and evaluation [8] [9]. A more detailed mapping of heart activity leading to the overall ECG cardiac cycle is shown in Figure 2.
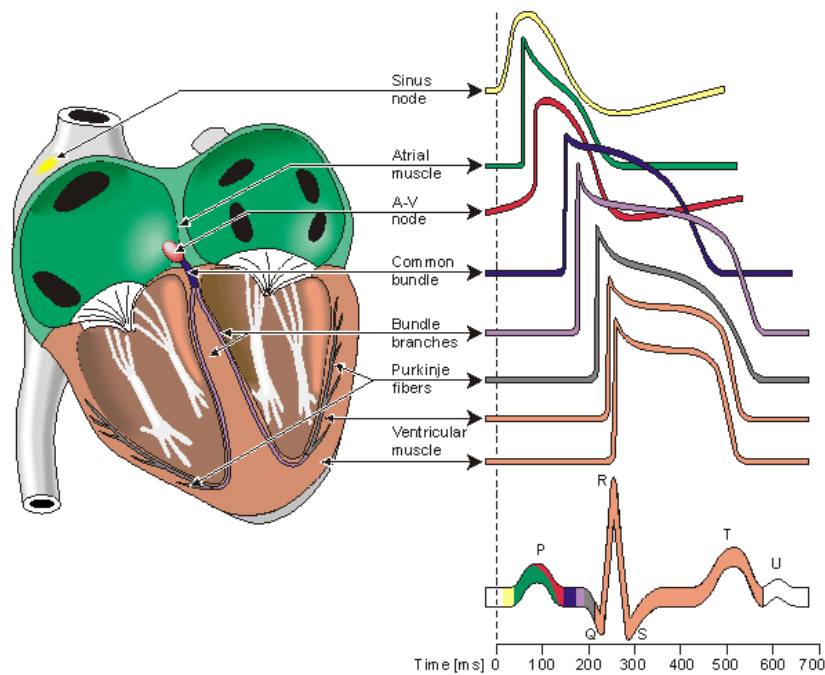


**Figure 2: The firing of signals from various heart location forming the ECG one cardiac cycle** [9]

7

Heart rate is measured by the time interval between two successive R peaks. The normal heart rate varies based on the age group as shown in Table 1.

**Table 1: Normal heart rate based on age** [10]

| Age | Heart Rates |
|---|---|
| Birth | 130 – 140 BPM |
| 1 to 12 months (infants) | 110 – 130 BPM |
| 1 year | 110 – 130 BPM |
| 2 years | 96 – 115 BPM |
| 3 years | 86 – 105 BPM |
| 14 to 15 years | 76 – 90 BPM |
| 19 years (adults) | 60 – 80 BPM |

## 2.1.1 ECG Electrodes Placement and Lead Systems

The shape of the ECG waveform is dependent on the placement of the ECG device's electrodes on the human body. The potential difference generated between two electrodes is known as a lead. A lead enables the medical professional to view the heart from a specific angle. Thus, a larger number of leads allow the medical professional to have a more comprehensive analysis. There are several types of ECG electrode placement or configurations, namely 1-lead for a single angle, 3-lead for 3 angles and 12-lead for 12 angles.

The bipolar 1-lead or single-lead ECG is formed by placing two electrodes on the left arm (LA) and the right arm (RA). It is known as Lead I. It is termed as bipolar because Lead I is sourced from their differential poles of its

respective electrodes. Thus, it is given by the voltage difference between the left arm (LA) and the right arm (RA) as shown in Equation 2-1.

$$Lead\ I = LA - RA \qquad (2-1)$$

$$Lead\ II = LL - RA \qquad (2-2)$$

$$Lead\ III = LL - LA \qquad (2-3)$$

The bipolar 3-lead ECG was proposed by Willem Einthoven in 1908 [9]. It is formed by placing three electrodes on the 3 limbs of the human body. With reference to the previous single-lead ECG, the 3-lead ECG configuration is formed by adding the left leg electrode. It is formed by Equation $2-1$ whereby Lead I is the voltage between the left arm and the right arm, Equation $2-2$ whereby Lead II is the voltage between the left leg and the right arm, Equation $2-3$ whereby Lead III is the voltage between the left leg and the left arm. These leads form the Einthoven's triangle as shown in Figure 3 and form the vertical perspective of the heart activities.
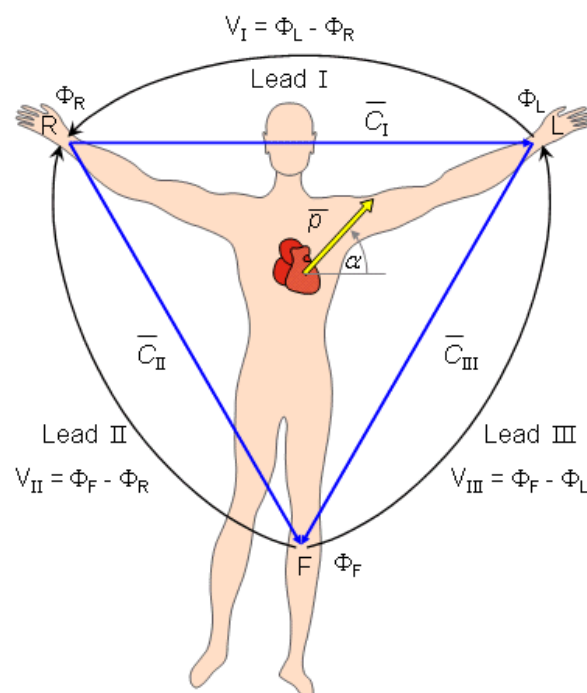


**Figure 3: Einthoven limb leads and Einthoven triangle** [9]

The 12-lead ECG is formed by the 3 bipolar limb leads, 3 unipolar augmented limb leads and the 6 unipolar chest leads. The 3 bipolar limb leads (Einthoven triangle) was described in the aforementioned paragraph. The remaining 9 unipolar leads are referenced to the Wilson Central Terminal (WCT). The WCT is formed by the average potential of the 3 limb leads.

The augmented limb leads consists of the aVR, aVL and aVF and they are derived using the LA, RA and LL as shown in Equation 2 – 4, Equation 2 – 5 and Equation 2 – 6:

$$aVR = RA - \frac{1}{2}(LA + LL) \qquad (2-4)$$

$$aVL = LA - \frac{1}{2}(RA + LL) \qquad (2-5)$$

$$aVF = LL - \frac{1}{2}(RA + LA) \qquad (2-6)$$
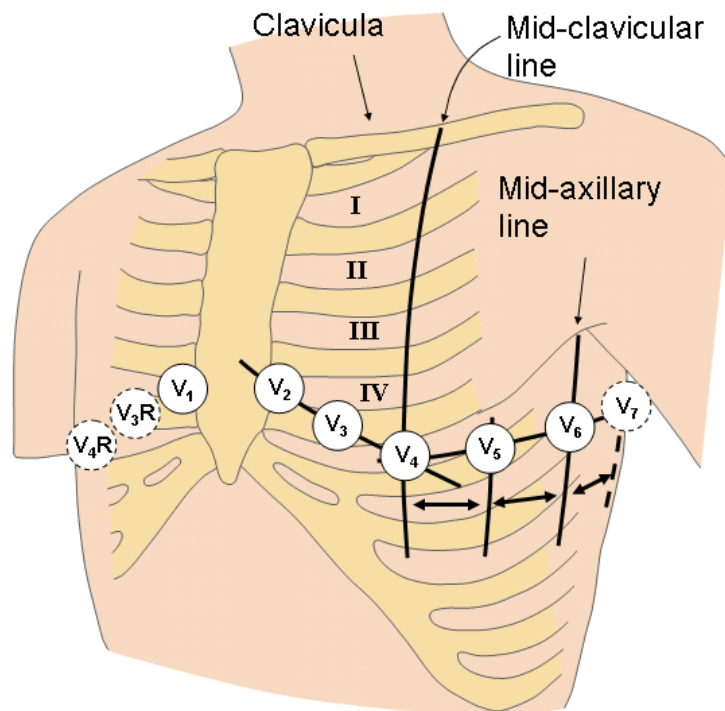


**Figure 4: Location of Lead V1 to V6 on a human subject** [9]

The chest or precordial leads consist of V1 to V6 and are placed as shown in Figure 4: The chest leads provide a horizontal perspective of the heart activities. The description of the each chest leads placement corresponding to its location is described in the Table 2. The mid-clavicular line and the $4^{th}$ intercostal space are the reference landmarks to align V2 to V4 whereas the mid-clavicular line and mid-axillary line are used for V4 to V6.

**Table 2: Location of Lead V1 to V6**

| Chest Lead | Location |
|:---:|:---:|
| V1 | $4^{th}$ intercostal space and on the right of the sternum |
| V2 | $4^{th}$ intercostal space and on the left of the sternum |
| V3 | Between V2 and V3 |
| V4 | $5^{th}$ intercostal space in between the mid-clavicular line |
| V5 | Horizontal of V4 |
| V6 | Horizontal of V5 |

### 2.1.2 Typical Architecture of a Wireless ECG Device
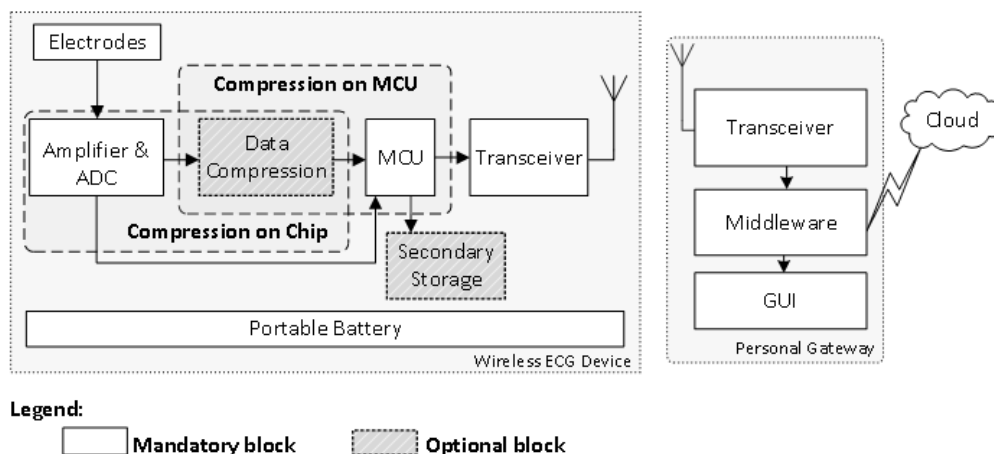


**Figure 5: General architecture of an end-to-end ECG system**

The general block diagram of an end-to-end ECG system is illustrated in Figure 5. It consists of a wireless ECG device for acquisition and transmission

11

of the ECG data and a personal gateway for display and relay of the ECG data to the cloud server or hospital. The personal gateway consists of a 'Transceiver' block for receiving ECG data, 'Middleware' block for signal processing and 'GUI' block for displaying the real-time ECG data.

The wireless ECG device consists of the 'Electrodes' block for conducting electrical signals from the human subject, the 'Amplifier & ADC' (AFE) block for transforming the analog ECG signals to the digital representation, 'Data Compression' as an optional block for reducing the number of digital data to represent a given ECG signal, the 'MCU' (microcontroller) block for overall system control and coordination, 'Secondary Storage' as an optional block for on-device ECG recording, 'Transceiver' block for transmitting the ECG data and receiving commands from the gateway via the wireless medium and light-weight 'Portable Battery' block to power-up the wireless ECG device.
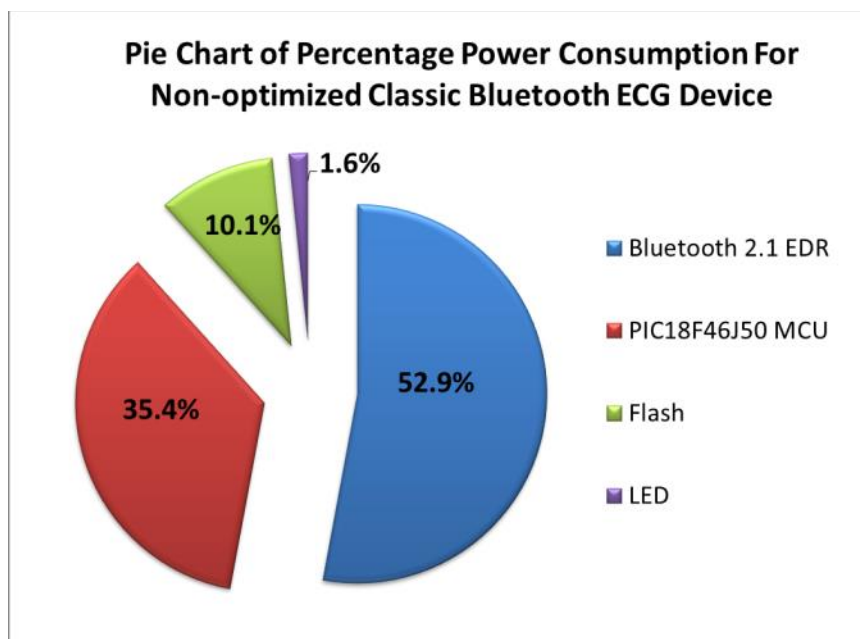


**Figure 6: Pie chart of power consumption for CB ECG device**

**Table 3: Tabulated power breakdown for non-optimized multi-lead ECG device**

|  | Current (mA) | Percentage |
|---|---|---|
| Bluetooth 2.1 EDR | 22.26 | 52.9% |
| PIC18F46J50 MCU | 14.89 | 35.4% |
| Flash | 4.23 | 10.1% |
| LED | 0.68 | 1.6% |
| Total | 42.06 | 100% |

However, research on biomedical sensor node has shown that during continuous ECG data transmission, the 'Transceiver' and 'MCU' block in wireless ECG sensor consumes more than 90% of the total power [11]. The power hotspot lies on the transceiver (70% to 80%) followed by the MCU (10% to 20%). From a system design using commercial off-the-shelf components, a wireless ECG device (also known as the CB ECG device) during continuous transmission can dissipate up to 42mA of current [6]. A more detailed analysis on [6] shows that the transceiver module takes up 52% of the overall power, followed by MCU at 35%, on-device flash at 10% and LED at around 2% as shown in Figure 6 and Table 3. This means that it can barely support 12 hours of continuous transmission on a typical light-weight battery capacity of 420mAh. A larger battery capacity (heavier) can be used but it will compromise the comfort of the user when worn [4]. Given the setback in battery density improvements and the need to deliver better performance, several embedded low-power technologies and techniques can be applied to reduce the overall power consumptions of the wireless ECG device.

### 2.1.3 Existing Solutions

An ambulatory electrocardiogram recorder ECGITM04 [12] was proposed for continuous offline monitoring for 7-days using a 9V primary battery. However, the size of the device (palm-size) may be obstructive and thus cannot be regarded as a wearable device. In addition, continuous real-time wireless transfer is not available and real-time signal processing is also not possible. As a response, a light-weight single-lead long playing cardio recorder (LPCR) was proposed [5]. It has an identical hardware as [6]. The device is attached to the human subject using adhesive. It can operate as an on-device ECG recorder (Holter) and can also transmit ECG data in real-time. The current drawn during on-device recording is less than 1mA enabling at least one month's worth of ECG recording. However, the current drawn during continuous transmission is not reported.

A light-weight wireless ECG plaster that is capable of transmitting to a ZigBee capable device for display is presented in [13]. The device is attached to the human subject using adhesive. It can last for 26 hours during continuous wireless transmission. The drawback of this proposal is based on the finding that low diagnostic yield (10% to 13%) was attributed to short monitoring time period of less than 48 hours, usually due to short battery life [3]. Furthermore, the use of ZigBee transceiver in [13] lacked support from commercial smartphone. AliveCor has developed a pocket-sized Universal Health Monitor (UHC) [14] for ECG monitoring. It can be attached to the back of any smartphone. The UHM has two exposed electrodes on the opposite surface. The close proximity supports the transmission of data from the UHC to the

14

smartphone via ultrasound. The smartphone picks up the ultrasound via its microphone. AliveCor claims that this technique consumes only ten percent than that of Bluetooth. The drawback of this design is that the pocket-sized UHC must be attached (close proximity) to the phone during monitoring; it is bulky and not meant for wearable continuous ECG monitoring. It is highly suited for occasional (event-based) monitoring.

**Table 4: Specifications of ECG devices**

| Technical Specifications | Long Playing Cardio Recorder [5] | ZigBee ECG Plaster [13] | AliveCor Universal Health Monitor[14] | WEB Biotechnology Spyder [15] |
|---|---|---|---|---|
| Size (mm) | 50 * 27 * 2 | 28 * 24 * 2 | 118 * 62 * 16.5 | 60 * 55 * 18 |
| Weight with batteries (g) | 45 | 25 | ECG sensor attached to smartphone | 48 |
| Transmission Technique | Recording: USB. Transmission: Classic Bluetooth | ZigBee | Ultrasound | Classic Bluetooth |
| Client Application | PC | PC | Smartphone | Smartphone |
| Usability | Adhesive on body | Adhesive on body | Event based on hand | Adhesive on body |
| No of Lead | 1 | 1 | 1 | 1 |
| Powered By | Li-Ion 3.7V 650mAH | Li-Ion 3.7V 650mAH | 3V CR2032 | 2 AAA battery |
| Duration stated in the documentation | ~30 days (recording) and 15 hours wireless | 26 hours | 6 months to 1 year | 3 days |
| Estimated current consumption @ battery capacity | 0.8mA (recording) and ~42mA (wireless) @ 650mAh | ~25mA @ 650mAh | Not available | 33.3mA @ 2400mAh |
| Sampling Rate | 256Hz | 100Hz | 300Hz | 250Hz |

Spyder [15] by WEB Biotechnology is a light-weight wireless ECG device for continuous ECG monitoring. It streams the ECG data to the smartphone via the Classic Bluetooth interface and then to the Cloud. It uses two AAA-size batteries (assume alkaline primary battery of 1200mAh each) which allow the device to operate for 3 days. The current consumption during continuous transmission is estimated at 33.3mA. Assuming that the capacity of the Li-Ion battery is 420mAh, this means that the continuous wireless streaming can barely last for 13 hours of operation. The battery life must last for at least 48 hours to obtain a clinical high diagnostic yield [3]. The commercial Spyder ECG device will be used as a benchmark for power improvements. The challenge is to lower the power consumption for continuous ECG monitoring on the wireless device. The specifications of these ECG devices are summarized in Table 4.

## 2.2    Requirements of an ECG Device

The purpose of the storyboard on Figure 7 is to describe on how the user (blue) interacts with the ECG device (square) through a gateway device (smartphone) whereby each scene describes certain features.

Allow me to tell you a story about John who is concerned on his health and has recently been feeling nauseous at certain times of the day. His doctor has prescribed an ECG device to monitor his conditions. Firstly, John turns on the ECG device by holding onto the button. He hears a beep indicating that the device has been turned on. In the second scene, John sees that the LED is blinking indicating to him that the electrode of the ECG device is not in

contact. During lead-off, the LED in the ECG device will blink simultaneously. In the third scene, John applies the ECG sensor onto his body. The LED on the ECG device stops blinking and turns solid. In the fourth scene, John takes out his smartphone and launches the ECG device's application. He selects the ECG Sensor A and presses the 'Start' button to begin the wireless ECG monitoring. In the fifth scene, the ECG data, heart rate, temperature, activity index, battery life, respiratory rate are transmitted from the ECG device and displayed. John can also be assured that the ECG device is functioning as the LED is glowing, indicating that the device has been applied correctly. In the final scene, John feels uncomfortable (heart palpitation or dizzy) and uses the event marker to indicate the region of interest. John's medical professional can then zoom into the region of interest for better clarity during consultation. John can press the disconnect button to stop monitoring. From the designer's viewpoint, the story implicitly requires the device's operating life during continuous monitoring to be as long as possible.
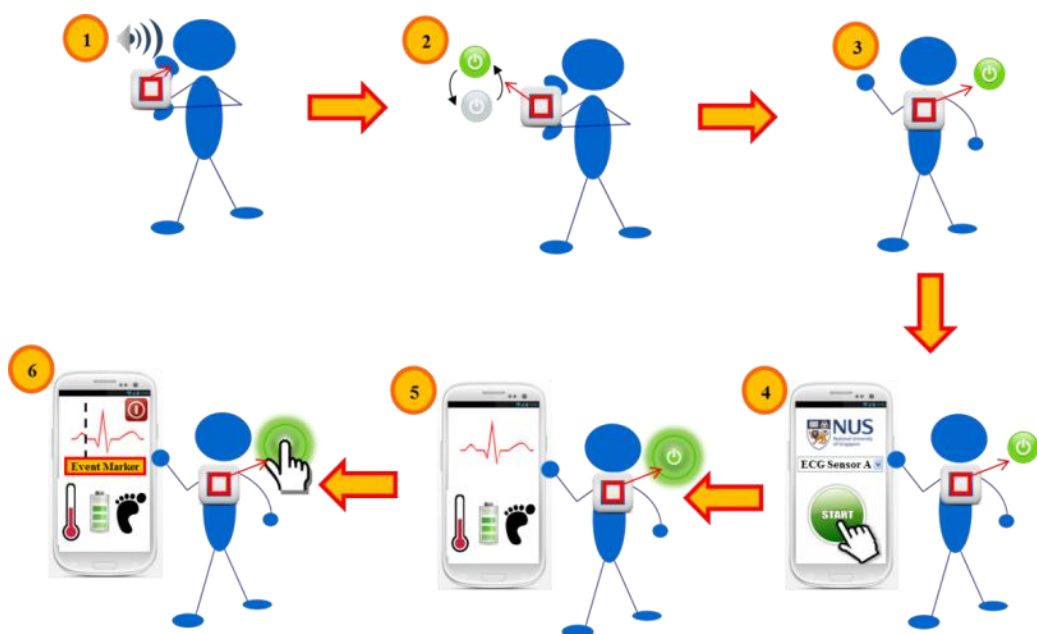


**Figure 7: Pictorial illustration of the storyline**

## 2.3    Requirements Capturing

Requirements capturing is a process of identifying the high-level system requirements (features) and partitioning them into tasks and subtasks. From the story described, the features are identified and converted into a list of requirements. These requirements also include the power reduction targets. The list of requirements will be categorized under mandatory and optional.

### 2.3.1    Mandatory Requirements

Mandatory requirements are requirements that have to be built into the final ECG device. It is prefixed with R.M.X.Y where 'R' represents requirements, 'M' represents mandatory, 'X' represents the requirements number and 'Y' represents the requirements sub-number.

**R.M.1. Display and Ensuring Accuracy of ECG AFE**

R.M.1.1. The ECG device must be able to stream at least 1-lead ECG signal to a smartphone in real-time.

R.M.1.2. The ECG sensor must be of resolution of at least 12 bits.

R.M.1.3. The sampling rate of the ECG sensor must be least 250Hz.

R.M.1.4. The heart rate derived from the waveform produced by the low-power wireless ECG device must be comparable to a commercial ECG device.

**R.M.2. ECG Lead Status Detection**

R.M.2.1. ECG chip should be able to detect lead-off.

R.M.2.2. The ECG device should alert the user during lead-off via the client application.

R.M.2.3. ECG device's LED toggles during lead-off.

R.M.2.4. ECG device's LED is solid during lead-on.

R.M.2.5. In addition to R.M.2.4, during ECG transmission, ECG device's LED will glow.

## R.M.3. Event Marker During ECG Monitoring

R.M.3.1. Button on the ECG device to indicate an event marker during the ECG monitoring.

## R.M.4. Wireless Transmission Between Smartphone and ECG device

R.M.4.1. The communication between the sensor and the personal gateway (smartphone) should be done via the wireless medium.

## R.M.5. Low-power During Continuous ECG Transmission

R.M.5.1. At least 3 times the power reduction as compared to the commercial wireless ECG device, Spyder.

## R.M.6. Rechargeable Battery

R.M.6.1 The ECG device should be powered up by a rechargeable Li-Ion battery of 420mA.

R.M.6.2 The rechargeable battery can be recharged when not in use.

## R.M.7. Low on the Shelf Battery Discharge

R.M.7.1 The battery drain when the device is not operational (sleep mode) should not go beyond 15µA.

### 2.3.2    Optional Requirements

Optional requirements are requirements that are not necessarily built into the final ECG system (ECG device and gateway). It is prefixed with R.O.X.Y where R represents requirements, O represents optional, X represents the requirements number and Y represents the requirements sub-number.

**R.O.1. Heart Rate Indicator**

R.O.1.1. The heart rate should be displayed on the client application.

R.O.1.2. The heart rate can be calculated from the ECG waveform via two successive RR peaks.

**R.O.2. Display Battery Life of the ECG device**

R.O.2.1 ECG device should support power monitoring.

R.O.2.2 Display the battery life on the client application.

**R.O.3. Measure The Activity Of The End-user**

R.O.3.1 To measure how active the user has been when the device is worn by the user.

**R.O.4. Ambient Temperature**

R.O.4.1 The ambient temperature is measured when the device is worn by the user.

**R.O.5. Fast Charge Of Less Than 2 Hours**

R.O.5.1 The charge time of the rechargeable battery should not exceed 2 hours.

**R.O.6. Respiratory Rate**

R.O.6.1 Measure the respiratory rate when the device is worn by the user.

**R.O.7. Storing the ECG Samples**

R.O.7.1 The ECG samples can be stored in the ECG device or on the smartphone.

## 2.4    Conclusion

The overview of the ECG system was introduced. The aim of this research is to reduce the power consumption of the ECG device during continuous ECG monitoring. The various types of existing ECG devices were compared and analyzed and the power reduction targets were proposed. The storyboard was introduced to describe the high-level features in the ECG system and its power requirements. After understanding the descriptive pictorial storyboard, the requirements were then listed. There are 7 mandatory requirements and 7 optional requirements.

# 3    Principles of Low-Power Embedded Design

The principles of low-power embedded design refer to the general techniques applied at system-level in order to reduce the power consumption of the ECG device. A review on how power is dissipated in a CMOS transistor can lead to the appreciation of the use of these techniques to achieve low-power in the ECG device.

There are two major sources of power dissipation in CMOS chips, dynamic power and static power [16]. Dynamic power dissipation is caused by the switching power where the load capacitor is firstly charged from low to high. During the high to low transition, this energy is discharged to the ground. This is illustrated in Figure 8.
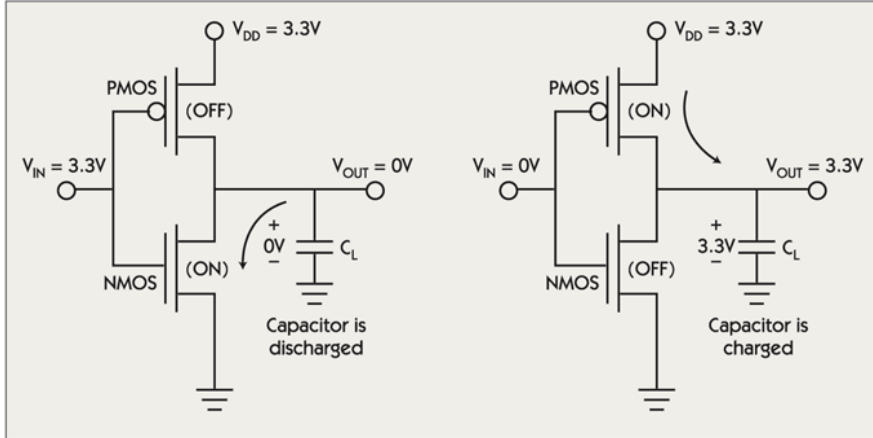


**Figure 8: High to low discharge (left) and low to high dissipation (right)** [4]

The load capacitance, $C_L$, is formed by combining the parasitic capacitance at the gate and the interconnections. The dynamic power model is given by Equation 3 – 1.

$$Power_{dynamic} = \alpha * C_L * V_{dd}^2 * f \qquad (3-1)$$

Whereby:

α is the switching probability from 0 to 1

$C_L$ is the load capacitance

$V_{dd}$ is the supplied voltage of the gate

f is the frequency of switching

In terms of static power dissipation, the CMOS is leaking current even when there is no switching activity. There are 2 main sources of static power dissipation, drain or source leakage and the sub-threshold leakage as illustrated in Figure 9. The former is due to the reverse-biased diode junction between the source/drain and the substrate. The latter is due to the inherent leakage of the drain-source current even when the gate source voltage is less than the threshold voltage. This inherent leakage increases along with the improvement of CMOS fabrication technology. The static power dissipation model is given by Equation $3 - 2$.

$$Power_{static} = I_{static} * V_{dd} \qquad\qquad (3 - 2)$$

Whereby:

$I_{static}$ is the static current dissipation

$V_{dd}$ is the supplied voltage of the gate
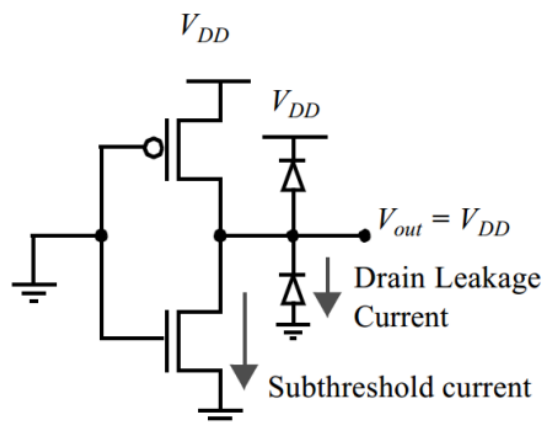


**Figure 9: Static power dissipation due to drain leakage current and sub-threshold current** [17]

23

Lowering the voltage supply, $V_{dd}$, has a quadratic reduction effect on the dynamic power dissipation in a CMOS chip as shown in Equation 3 − 1 [17] [16]. Equation 3 − 1 also shows that frequency (f) is a linear function to the dynamic power dissipation. Frequency scaling is a technique to switch or alter the MCU's clock frequency. When there is no task, the frequency is lowered and when a new task arrives, the clock frequency is increased.

From an embedded systems design perspective, the $\alpha$, $C_L$ from Equation 3 − 1 are parameters related to the transistor level design and it cannot be tuned at the PCB level or firmware (systems level perspective). On the other hand, the $V_{dd}$ and frequency can be configured and controlled from the PCB circuit level and MCU respectively. This means that the ability to lower the voltage supply, $V_{dd}$, and the frequency scaling technique at system-level can help to reduce the dynamic power dissipation.

Toggling between active/idle modes is mainly used to reduce the dynamic power dissipation. The main objective of this optimization technique is to enable the device to remain in idle mode (standby) for as long as possible [18]. In idle mode, only static power dissipation occurs. However, in active mode, both static and dynamic power dissipation occurs at the same time as illustrated in Figure 10.
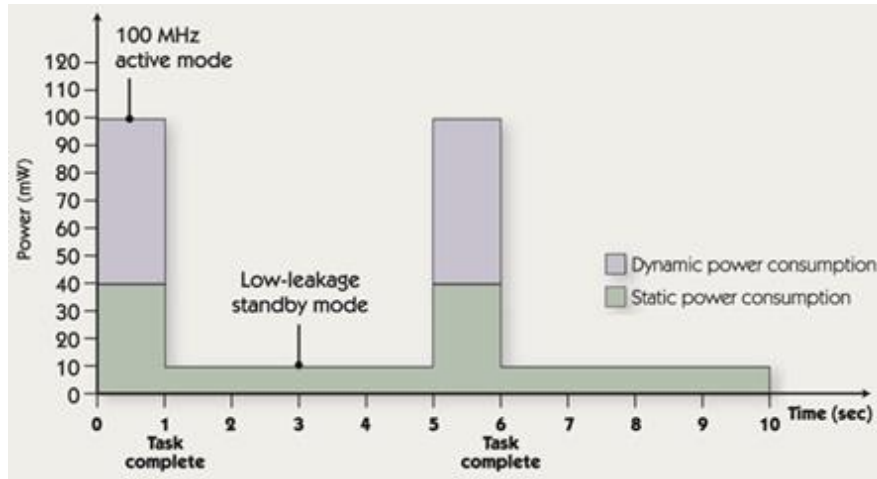
**Figure 10: Static and dynamic power dissipation against time** [4]

Assuming that the device is an MCU, this means that the MCU will complete the task at hand (100 MHz active mode) before going back to idle mode (low-leakage standby mode). These modes require run-time power management features within the low-power processor idle modes. Fast wake-up time from idle mode to active mode must be supported for this power saving functionality. This technique can also be supported by a buffer to store temporary data and bursting once the buffer is full in order to reduce overhead. For example, the MCU in the ECG device can acquire multiple samples into its SRAM before transmission.

Power gating is a technique used in integrated circuit design to reduce static power dissipation by shutting off the current to blocks of the circuit that are not in use. This technique can be applied on various levels of granularities such as on the IC component level. Since we are designing at the system level, this technique can use a power management chip to gate or cut the main power supply rail. Therefore, the peripherals connected to the power supply rail such as the microcontroller, AFE, transceivers are completely unpowered. This

technique is designed to minimize leakage power during long-term power down or when the device is kept on the shelf.

In terms of the low-power design on both hardware and software, embedded hardware software co-design calls for the need for system partitioning to map the intended features to hardware or software, with the intention to get the best out from both realms [19]. Thus, system partitioning requires careful study and understanding of the hardware and software to meet the power constraints. As described two paragraphs ago, the hardware and software must work hand-in-hand for the toggling between the active and idle mode in order to reduce dynamic power dissipation; quick toggling must be supported by the hardware MCU and the switching is controlled by the software. In another example, a less power optimized approach of reducing static power dissipation during long-term power down would be to emphasize on the software's flexibility (MCU's firmware) by putting all components to sleep mode instead of investing on a hardware power gated IC.

## 3.1    Selection of Wireless Transceiver Standard

Wireless transceivers consume more than 50% of the overall power in a typical wireless sensor [6] [11]. Therefore, the selection of wireless transceiver interface plays a crucial role towards the overall power consumption of the ECG device. The IEEE 802.11 (Wi-Fi) and the IEEE 802.15 (Wireless Personal Area Network - WPAN) working group are the two major players in wireless technology. Under the WPAN umbrella, there are IEEE 802.15.1 (dormant and currently maintained by the Bluetooth Special Interest Group

(SIG)) Bluetooth Standards, IEEE802.15.2 focusing on the co-existence of 802.11 and 802.15, IEEE 802.15.3 and IEEE 802.15.4 for low-power WPAN and IEEE 802.15.6 Wireless Body Area Networks (WBAN) for body area communication.

**Table 5: Working groups of IEEE 802 standards**

| Name | Description |
|---|---|
| IEEE 802.11 | Wireless LAN (WLAN) or Wi-Fi |
| IEEE 802.15 | Wireless Personal Area Network (WPAN) |
| IEEE 802.15.1 | Bluetooth Certifications (dormant) – actively maintained by Bluetooth SIG |
| IEEE 802.15.2 | IEEE 802.15 and IEEE 802.11 co-existence |
| IEEE 802.15.3 | High-Rate WPAQN (HR-WPAN) |
| IEEE 802.15.4 | Low-Rate WPAN (LR-WPAN) |
| IEEE 802.15.6 | Wireless Body Area Networks (WBAN) |

These standards are usually distinguished from each other by power consumption, data rate and device cost. These wireless technologies have also been used in environmental monitoring and intelligent control, logistics, medical, healthcare, etc. In recent years, WBAN has gained much interest in the research community for the development of low-power wearable healthcare devices. However, it lacked commercial hardware support for implementation of a low-power wireless ECG device. Throughout this thesis, the IEEE 802.11 (Wi-Fi), Bluetooth SIG and IEEE 802.15.4 standard will be further discussed because these standards are more widely adopted by commercial transceiver manufacturers.

### 3.1.1 Wi-Fi (IEEE 802.11)

IEEE 802.11 is commonly known as Wi-Fi or Wireless Fidelity. IEEE 802.11 communication interface is commonly available in laptops, smartphones, etc. IEEE 802.11 provide 2 topologies, namely an ad-hoc mode between two stations (STAs) and infrastructure mode whereby STAs are connected to an access point (AP) forming a star topology.

**Table 6: Comparison of IEEE 802.11 standards**

|  | 802.11b | 802.11a | 802.11g | 802.11n |
|---|---|---|---|---|
| Frequency Band | 2.4GHz | 5GHz | 2.4GHz | 2.4/5GHz |
| Max data rate | 11Mbps | 54Mbps | 54Mbps | 600Mbps |

Ever since the conception of IEEE 802.11 standards, a number of improvements and functionalities have been added namely 802.11b, 802.11a, 802.11g and 802.11n. A comparison of their key features can be seen on Table 6. These standards can operate on 2.4GHz or 5GHz frequency band or spectrum. The maximum data rate has gradually improved from 11Mbps to 300Mbps. However, the power consumption of the IEEE 802.11 technology is very high, up to 330mW (100mA at 3.3v) which is typically not suitable for a battery powered wearable ECG device [20][21].

### 3.1.2 ZigBee (IEEE 802.15.4)

The IEEE 802.15.4 task group joined hands with the ZigBee Alliance to create a low-power WPAN standard nicknamed ZigBee. As shown in Figure 11, the IEEE 802.15.4 task group focuses on the physical (PHY) and medium

access control (MAC) layer. On the other hand, the ZigBee Alliance focuses on the higher layer stack and the application layers.

The ZigBee topology is made up of a sole coordinator for network and management functions, router for hopping around ZigBee networks and end devices which are usually the sensor end nodes. However, this standard is not available as a common interface for the smartphones. The typical ZigBee power consumption is about 100mW (3.3v by 30mA) [13].
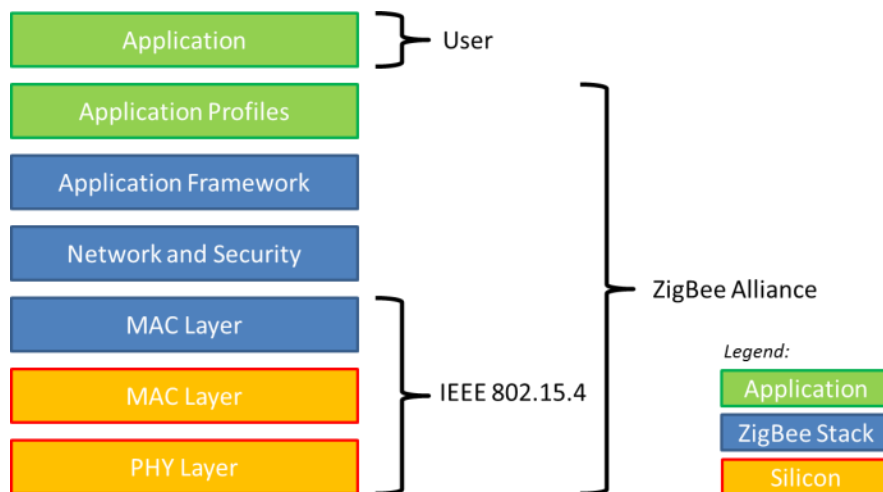


**Figure 11: ZigBee protocol stack**

The ZigBee Specifications IEEE 802.15.4 is summarized in Table 7. The ZigBee Specifications operates on 3 different frequency bands depending on the region. In Europe, America and worldwide, ZigBee operates at 868MHz, 915MHz and 2.4GHz respectively. The frequency band has a significant impact on the maximum data rate. For regions with lower frequency band such as Europe and America, the maximum data rate is 20kbps and 40kbps respectively. On the other hand, regions aside from Europe and America (worldwide) can operate in the 2.4GHz frequency band enabling data rate of up to 250kbps. The typical indoor range of ZigBee ranges from 10m to 100m

depending on the hardware transmission power and receiver sensitivity. However, ZigBee may consume lower power than Wi-Fi protocols but is less appealing for a wearable wireless ECG device because of the lack of support of ZigBee protocols in smartphone.

**Table 7: General ZigBee specifications**

| Technology | ZigBee | | |
|---|---|---|---|
| IEEE Specifications | 802.15.4 | | |
| Frequency Band | 868MHz | 915MHz | 2.4GHz |
| Region | Europe | America | Worldwide |
| Maximum Data Rate | 20kbps | 40kbps | 250kbps |
| Typical Indoor Range | 10m to 100m | | |

### 3.1.3  Classic Bluetooth (2.1 EDR) and BLE (Bluetooth 4.0)

Bluetooth is maintained by the Bluetooth Special Interest Group (SIG). Its main objective is to provide a short range ad-hoc networking without the need of a dedicated infrastructure. There are two popular interfaces by the Bluetooth SIG, Bluetooth 2.1 Enhanced Data Rate (EDR)/Classic Bluetooth and Bluetooth Low Energy (BLE). Classic Bluetooth is designed for high throughput requirements such as a 12-lead ECG but BLE is designed for low-power (by sacrificing data rate and frequency of transmission). BLE is appealing for low data rate wireless sensor network and can be pushed to support real-time streaming capabilities for limited lead ECG devices [22][23]. However, both of these standards are not compatible to one another.

A comparison between Classic Bluetooth and BLE is tabulated on Table 8. The Classic Bluetooth has a more superior data rate, throughput and open air distance due to the ability to transmit data more frequently and at a much larger power than the BLE devices; theoretically 2 times the peak current than BLE. BLE is designed to quickly establish connectivity from a disconnected state. This is about 17 times faster than its predecessor.

The Bluetooth interface is well adopted by the smartphone manufacturers. In terms of Classic Bluetooth, the smartphone manufacturers have supported several common Bluetooth data transfer profiles such as Simple Secure Pairing (SSP), Serial Port Profile (SPP) [24]. Recently, the support for BLE enabled smartphone has increased and its standardized profiles has been adapted by various smartphone manufacturers. In the case of the streaming nature of an ECG payload, notifications profile is used for data streaming between the ECG device and the smartphone.

In terms of robustness, the Classic Bluetooth supports forward error correction (FEC) mechanisms whereas BLE relies on a 24-bit cyclic redundancy check (CRC). Forward error correction is a technique used to correct the received data at the receiving end (transmitted over unreliable channel) with the aim of avoiding retransmission. This comes at a cost of encoding redundancies in its frame payload prior to transmission. Its ability to detect and correct errors is dependent on its encoding scheme. On the other hand, BLE relies on CRC to ensure the integrity of the data received. Retransmission will happen when the CRC calculated by the receiver (via the

received frame) doesn't match the CRC that was transmitted. Furthermore, both the Classic Bluetooth and BLE use the adaptive frequency hopping to combat the coexistence interference in a congested frequency spectrum such as the 2.4GHz. In summary, the Bluetooth interface is preferred because it is widely adopted by smartphone manufacturers (in contrast to the ZigBee protocol) and it has a fair current consumption (in contrast to the Wi-Fi protocol).

Table 8: General Bluetooth specifications

| Technical Specifications | Classic Bluetooth Technology | Bluetooth Low Energy |
|---|---|---|
| Open Air Distance | 100 m | 50 m |
| Over The Air Data Rate | 1–3 Mbit/s | 1 Mbit/s |
| Theoretical Application Throughput | 0.7–2.1 Mbit/s | 0.27 Mbit/s |
| Class (maximum permitted power) | Class 1 – 100mW ~100m<br>Class 2 – 2.5mW ~10m<br>Class 3 – 1mW ~1m | Typ. 1mW (10mW max) [25] |
| Peak Current Consumption | <30 mA | <15 mA |
| Latency (from a non-connected state) | Typically 100 ms | 6 ms |
| Data Transfer Profiles | SPP (Serial Port Profile) | Notification Profile |
| Robustness | Adaptive frequency hopping, FEC | Adaptive frequency hopping, 24-bit CRC |

## 3.2    ECG Compression For Power Reduction

Wireless transmission consumes substantial amount of power in an ECG devices. [11] and [6] claimed that up to 50% of power dissipation for a typical smart sensor node is attributed to wireless transmission. Data compression techniques via a data compressor can be used to eliminate redundancies and

reduce the size of the ECG data for wearable sensors. The reduction in size reduces the rate for wireless transmission, which leads to lower power dissipation. In addition, compression also helps to reduce the size of storage requirements (MCU's SRAM and flash). Thus, the reduction also helps to reduce the overall cost and size of the ECG device.

However, in order to find significant gains using the compression technique, the power consumed by the compressor, $P_{comp}$ should be lower than the prospective power savings obtained by the use of compression as shown in Equation $3-3$ [26].

$$P_{comp} \ll P_{TX} - \frac{P_{TX}}{BCR} \qquad (3-3)$$

Whereby:

$P_{TX}$ is the static current dissipation

BCR (Bit Compression Ratio) is the performance of the compression. BCR indicates the number of uncompressed bits that can be represented by a compressed bit. It is given below as:

$$BCR = \frac{No\ of\ uncompressed\ bits}{No\ of\ compressed\ bits} \qquad (3-4)$$

There are two types of compression techniques, lossy and lossless. These techniques will be discussed in the following sub-sections.

### 3.2.1   Lossy Compression

Lossy compression means that the compressor removes information that is deemed insignificant or redundant in order to reduce the size of the data. However, during the decompression stage, reconstruction to the original signal cannot be done. Previous research has shown that lossy compression can achieve high compression ratio of about 2 to 10 times [27].

Lossy compression can be performed by subsampling and introducing quantization. Lossy compression algorithms can be done in time and frequency domain. Examples of time domain algorithms are amplitude zone time epoch coding (AZTECH) as shown in Figure 12, FAN Algorithm, turning point algorithm, etc [28] [29] [30]. Examples of frequency domains are Karhuen-Loeve-Transform (KLT), Discrete Cosine Transform (DCT), etc [31] [32].
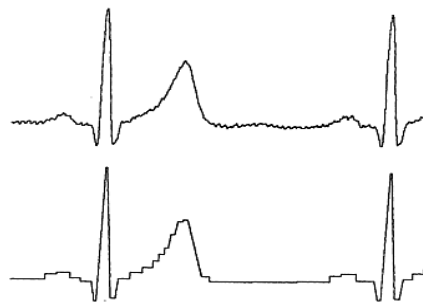


**Figure 12: Original ECG signal vs lossy AZTECH signal.**

### 3.2.2   Lossless Compression

In lossless compression for ECG data, a predictor is usually used to remove any redundancy in the incoming signals. The resulting signal is known as the entropy. The entropy signals are further evaluated using entropy coding

techniques in order to reduce the number of bit representations. The general flow is shown in Figure 13.
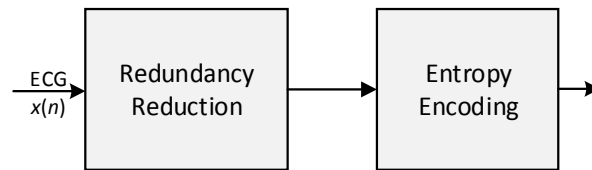


**Figure 13: Lossless ECG encoding generic block diagram**

The lossless compression can achieve about 1 to 3 times without losing the integrity of the original signal. Therefore, lossless compression is favoured over lossy in the biomedical arena as it guarantees the fidelity of the signal. However, the compression ratio cannot be guaranteed. Examples of lossless compression algorithms are:

❖ The Short Term Predictor: In this technique, the short term predictor is used to predict the next sample based on its previous samples. It takes advantage of the relatively slow varying ECG signal with high correlation through spatial analysis [33]. The low-complexity lossless algorithm used in our design falls along this category and will be discussed in detail in Section 6.2.2.

❖ The Long-Term Predictor: In this technique, the long-term predictor is used to detect the past ECG features (R-peak of the QRS complex) and aligns itself to the incoming QRS complex. It leverages on the temporal knowledge that the previous QRS complexes are highly identical to the current QRS complex [34]. After the redundancy reduction via prediction, techniques such as Huffman Coding and Golomb Coding can be used to represent the signal in a shorter or smaller size.

❖ Template Extraction and Coding: In this technique, standard templates of ECG segments (P, QRS and T waves) are used and compared against the incoming data to form the residue [35]. The residue can then be truncated by the Huffman coding to form the compressed signal. However, the computational complexity is deemed to be relatively high.

❖ Transform Domain Techniques: This technique involves the transformation of signals from one domain to another to reduce redundancy. The redundancy reduction is performed by a domain transform function such as Burrows Wheeler Transform (BWT) [36]. After that, linear prediction and arithmetic coding techniques can be applied to reduce the overall size of the compressed signal. The transform domain technique is relatively expensive in terms of computational resources.

## 3.3    Conclusion

The principles of low power design reflect on the two major sources of power dissipation on the CMOS transistor, the static and the dynamic. At system level through power profiling, the dissipation is concentrated at the transceiver. Based on the requirements and tradeoff analysis, the Bluetooth standard is chosen and the compression technique can be used to reduce the overall power of the wireless ECG device.

# 4 Hardware Platform for Wireless ECG Device

## 4.1 Power Management Integrated Circuit

Power management integrated circuit (PMIC) is an integrated circuit that can be used to manage power requirements in a battery operated device. The PMIC in the ECG device regulates the voltage supply to the components and provides additional features such as battery charging.

The Linear Technology LTC3553 Micropower USB Power Manager With Li-Ion Charger is an integrated power management cum battery charger IC for single-cell Li-Ion battery application [37]. It has a low dropout regulator (LDO) and a high-efficiency buck switching regulator which is supported by a push button controller.

The integration of the push button controller in the PMIC allows the use of ultralow quiescent state whereby all power supplies are disabled making it ideal for product shipping or long-term storage. Figure 14 shows the plot of battery drain current (quiescent) against time. At 'hard reset' and 'buck and LDO off', the battery drain current at room temperature ($21^{\circ}$C) is about $0.2\mu$A and $3\mu$A respectively. The LTC3553 also supports Li-Ion battery charging on the USB power supplies.
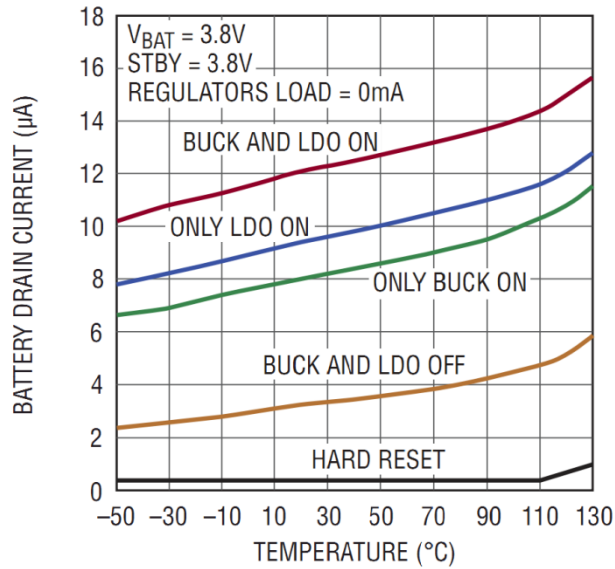
**Figure 14: Plot of battery drain current (quiescent) against time** [37]

## 4.2 ECG Sensors

ECG sensors are used to acquire the bio-potential of a body. The ADS192R by Texas Instruments is a two-channel 24-bit delta-sigma ADC for bio-potential measurements [38]. It is able to measure ECG and bio-impedance. The two channels can be configured for ECG measurements or respiration bio-impedance measurements. It has two power inputs for the analogue and digital ranging from 2.7V to 5.25V and 1.7V to 3.6V respectively. The analogue is powered by a 3V LDO whereas the digital is powered by a 2.2V supply. Data acquired by ADS1292R can be transfer via the serial peripheral interface (SPI) interface. The SPI reads and writes can be done at clock rates of up to 4MHz. The sampling rate can range from 125SPS (samples per second) to 8kSPS (kilo samples per second). For our ECG device, the sampling rate is configured to 250SPS.
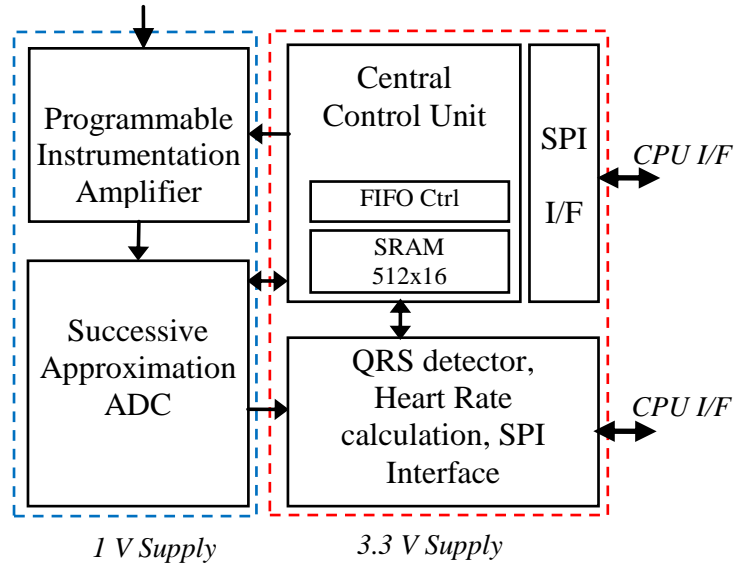
**Figure 15: Block diagram of the NUS ECG Chip with buffer mode** [6]

The NUS ECG chip with buffer mode is a 12-bit single-lead ECG (2 bytes per sample) with an 8k bit of SRAM [6]. The SRAM can buffer for about 2 seconds worth of ECG samples at a sampling rate of 256Hz. This buffered mechanism is solely designed to enable longer inactivity of MCU resulting to more power savings. The ECG front-end architecture is designed as shown in Figure 15 [6]. It integrates an instrumentation amplifier, a band-pass filter, a successive approximation register (SAR) analog to digital convertor (ADC), a real-time QRS detection, an on-chip SRAM and FIFO for buffering the ECG signal, a central control unit, a serial peripheral interface (SPI), and an on-chip clock. The instrumentation amplifier is programmable for different gain settings, which maximizes the dynamic range of the system.

The tunable band-pass filter serves as direct current (DC blocking and anti-aliasing). The low pass cut-off frequency can be tuned to match the change of sampling rate. A 12-bit SAR ADC is used to maintain good signal resolution. The 8-kbit SRAM and First-In First-Out (FIFO) facilitate the data storage and

synchronize with a faster external MCU clock. The central control unit is used to decode incoming MCU commands and control each subsystem in the chip. Voltage domains of 1.0V and 3.3V are designed within to ensure maximum power savings. The measured power consumption of the chip is 2.3μW.

The system block diagram of the NUS ECG chip with Data Compression is shown in Figure 16 [27]. The front-end consists of 4 recording channels, a multiplexer (MUX) and a 12-bit successive approximation (SAR) ADC. The backend includes a lossless compression block for compression, a real-time clock (RTC) module, and a SPI interface for inter-chip communication. The lossless compression algorithm and its performance will be discussed in Section 6.2.2. The driven-right-leg (DRL) is included to improve the ECG signal quality and the reduction of 50- or 60-Hz power-line noise. In addition, an internal low-power 32.768 kHz crystal oscillator driver is implemented to reduce external components counts on the PCB. The whole chip is designed to work at 2.4V to 3.0V power supply.
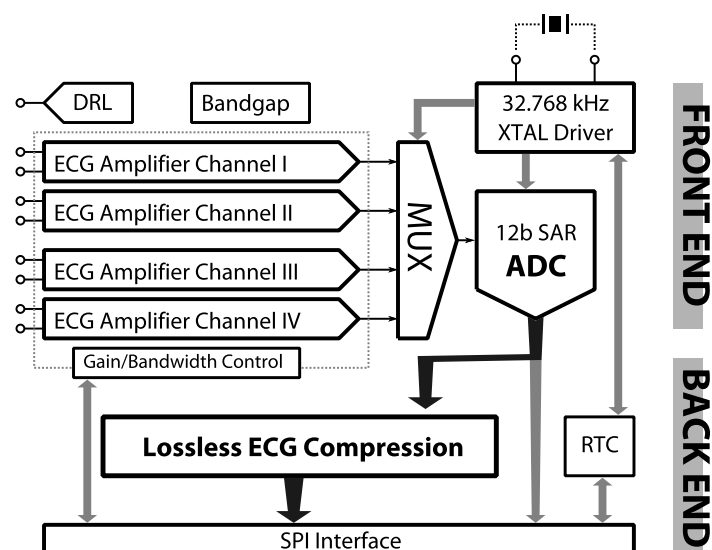


**Figure 16: Block diagram of the NUS ECG Chip with data compression** [27]

The comparison between the 3 ECG sensors (Texas Instruments ADS1292R, NUS ECG Chip with Buffer Mode and NUS ECG Chip with Compression mode) are tabulated in Table 9. The TI ADS1292R is a dual channel ECG sensor which is able to support a wide range of sampling rate starting from 125SPS to 8kSPS at 24 bits per sample resolution. The NUS ECG Chip with Buffer Mode (single channel) and Compression Mode (4 channels) is able to support a sampling rate of 256SPS and 256SPS to 512SPS respectively. The resolution supported by both the NUS ECG chips falls at 12-bits per sample.

**Table 9: Comparison between ECG Sensor Chips**

|  | TI ADS1292R [38] | NUS ECG Chip with Buffer Mode [6] | NUS ECG Chip with Compression Mode [27] |
|---|---|---|---|
| Number of Channels | 2 | 1 | 4 |
| Sampling Rate | 125SPS – 8kSPS | 256SPS | 256SPS – 512SPS |
| Resolution | 24-bit | 12-bit | 12-bit |
| Buffer Mode | Absent | Present | Absent |
| Compression Mode | Absent | Absent | Present |
| Respiratory Rate | Present | Absent | Absent |
| Peripheral Interface | SPI | SPI | SPI |
| Power Consumption per channel | 335µW | 2.3µW | 8µW |

The buffer mode (in-built SRAM) is only supported by the NUS ECG Chip with Buffer Mode whereas the compression mode is only supported by the NUS ECG Chip with Compression Mode. The TIADS1292R is able to perform bio-impedance measurement. The bio-impedance measurement can be later used to derive the respiratory rate. All the ECG sensor chips use the

standardized SPI protocol for data transfer and communication. This means that the ECG chips can be interchanged with minimal PCB changes. It is noted that the commercial TI ADS1292R has much larger power consumption per channel than the NUS chips.

## 4.3    Transceiver Module

Transceiver module is a component that can be used by the ECG device to transmit data. Referring to transceiver characteristics in Section 3.1 and the requirements in Section 2.3, the Bluetooth standard is preferred over Wi-Fi and Zigbee because of it has lower power consumption and it is also compatible for smartphone handsets. Two Bluetooth transceiver modules that meet the above criteria will be introduced in the following sub-sections.

The Bluegiga WT-12 is a Classic Bluetooth (Bluetooth 2.1 EDR) module that is bundled with a Bluetooth radio transceiver and an on-chip microcontroller named BlueCore 4 [39]. The microcontroller within the module acts as an interrupt controller and schedules the Bluetooth stack via an event timer. It also has an integrated chip antenna. The module can be interface with an external MCU via the SPI or USB interface. SPP profile is supported to enable serial communication with the smartphone. The main advantage of using WT-12 lies at the hassle free inbuilt antenna within the module. However, the disadvantage lies at its physical size being larger than KC-22.

The KC-22 by KC Wirefree is a micro size (13.4mm x 11.3mm x 2.0mm) Classic Bluetooth (Bluetooth 2.1 EDR) module embedded with a Cambridge Silicon Radio (CSR) BlueCore 4 which is identical to the WT-12 module [40]. In addition, the Bluetooth SPP profile is supported to allow serial communication with the smartphone. It also supports UART and SPI protocol for serial communication with the MCU. However, it does not have an inbuilt antenna which may turn out to be unfavourable to those who are not familiar with antenna design.

**Table 10: Comparison between WT-12 and KC-22**

|  | **Bluegiga WT-12** [39] | **KC Wirefree KC-22** [40] |
|---|---|---|
| Bluetooth Technology | Bluetooth 2.1 EDR | Bluetooth 2.1 EDR |
| Class | Class 2 Radio | Class 2 Radio |
| Transceiver Chipset | Cambridge Silicon Radio (CSR) BlueCore4 | Cambridge Silicon Radio (CSR) BlueCore4 |
| Size (Length x Width x Thickness) | 15.6mm x 14.0mm x 2mm | 13.4mm x 11.3mm x 2.0mm |
| Profile Support | SPP (Serial Port Profile) | SPP (Serial Port Profile) |
| Communication Interface | UART and USB | UART and SPI |
| UART Baud Rate | 921600 | 921600 |
| Embedded module antenna | Included | Absent |

A comparison between the two Classic Bluetooth modules, Bluegiga WT-12 and KC Wirefree KC-22 is shown in Table 10. It can be seen that both WT-12 and KC-22 modules are similar in terms of Bluetooth Technology, Class, Transceiver Chipset, Profile Support and UART Baud Rate. This similarity is mainly due to the use of the same transceiver chipset (Cambridge Silicon Radio (CSR) BlueCore 4). The main difference lies at the size of the module where WT-12 is larger than KC-22 as it has an embedded module antenna.

WT-12 is catered for PCB designers who are not concerned about the PCB size.

## 4.4    Accelerometer

The accelerometer is a component to measure the acceleration of a moving or vibrating body. The unit of measure is known as proper acceleration or g-force at 9.81 m/s$^2$. The output of the accelerometer in the ECG device can be used to measure the activity of a body.

The MMA8452Q by Freescale Semiconductor is a low-power 3-axis accelerometer with 12 bits resolution [41] . It has selectable scales of ±2g or ±4g or ±8g. It also has a sampling rate from 1.56Hz to 800Hz. Its current draw ranges from 6µA to 165µA. It has two programmable interrupt pins assigned to an embedded digital signal processing block allowing free-fall detection, transient detection, tap detection, etc. It is interfaced to the microcontroller via an I$^2$C digital output.

## 4.5    Microcontroller

Microcontroller is used to manage the overall operations of the ECG device. This subsection introduces two types of microcontroller that can be used for the wireless ECG device.

### 4.5.1 Microchip PIC18F46J50

The Microchip PIC18F46J50 is a 16-bit microcontroller with CPU frequency of up to 12MHz [42]. It has various power management modes such as idle mode with current draw of about 2.3µA. Idle mode refers to the MCU power saving state where the CPU is turned off and the peripherals remains active. It has wake up time of about 1.5µs. It supports 2 serial ports which can be programmed as SPI interface or $I^2C$. It has a UART communication interface that can go up to a baud rate of 921600. It has analogue to digital subsystem for voltage potential measurement. In terms of peripheral interface, it has an inbuilt USB 2.0 Full-Speed (12 Mbps) compliant interface. Table 11 summarizes the configurations of PIC18F46J50.

### 4.5.2 8051 MCU on Texas Instruments CC2540

The CC2540 is a low-power System-on-chip (SoC) for Bluetooth Low Energy (BLE) application [43]. The SoC consists of an enhanced 8051 MCU with 8kB of SRAM. The CPU frequency of the 8051 MCU can go up to 32MHz. It has a fast wakeup time (less than 4µs) from sleep mode. It has 2 serial ports that can be configured as SPI or UART (up to 921600 baud rate). However, hardware $I^2C$ is absent so software $I^2C$ can be supported if required. It has analogue to digital subsystem for voltage potential measurement. In terms of peripheral interface, it also has an inbuilt USB 2.0 Full-Speed (12 Mbps) compliant interface. The SoC has an integrated BLE transceiver. The CC2540 is accompanied by a BLE stack for quick BLE application development. Table 11 tabulates the typical configurations of the Texas Instruments CC2540.

The CC2540's BLE stack is divided into two portions, the controller and the host as shown in Figure 17. The controller is responsible for running the physical layer packets of the stack which requires hard real-time timings. The physical layer (PHY) is running at 1Mbps adaptive frequency hopping operating in the 2.4GHz band. The link layer (LL) manages the 5 states of the radio, advertising, scanning, standby, initiating and connected. The host-controller interface (HCI) is a bridge between the host and the controller. The interface can be a serial communication, USB or software APIs. The HCI interface can be deactivated in our case since the host and the controller are on the same MCU.
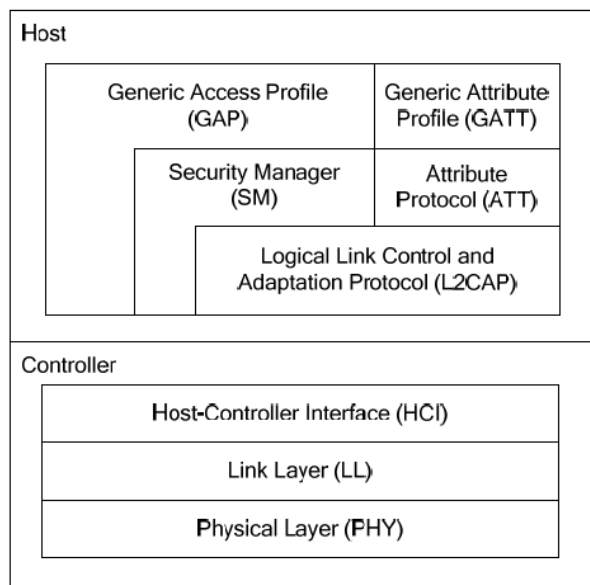


**Figure 17: BLE stack protocol** [44]

Within the host, the logical link control and adaptation protocol (L2CAP) is responsible for encapsulating the higher level data and responsible for reliable end to end communications. The security manager (SM) provides secure data transfer such as paring and key exchange. The generic access protocol (GAP) provides fundamental inter-device communication such as device discovery

and access to the application layer. It is also responsible for initiating security features. The notification profile in the application layer can support about 20 bytes of payload for a single frame transmission. The attribute protocol (ATT) provides device attributes based on whether it is a server or client. The Generic Attribute Profile (GATT) defines a service framework to access the ATT layer and interfaces for data communication between two BLE devices. In addition, there are 2 major parameters within the stack that affects the power consumptions, connection interval and slave latency.
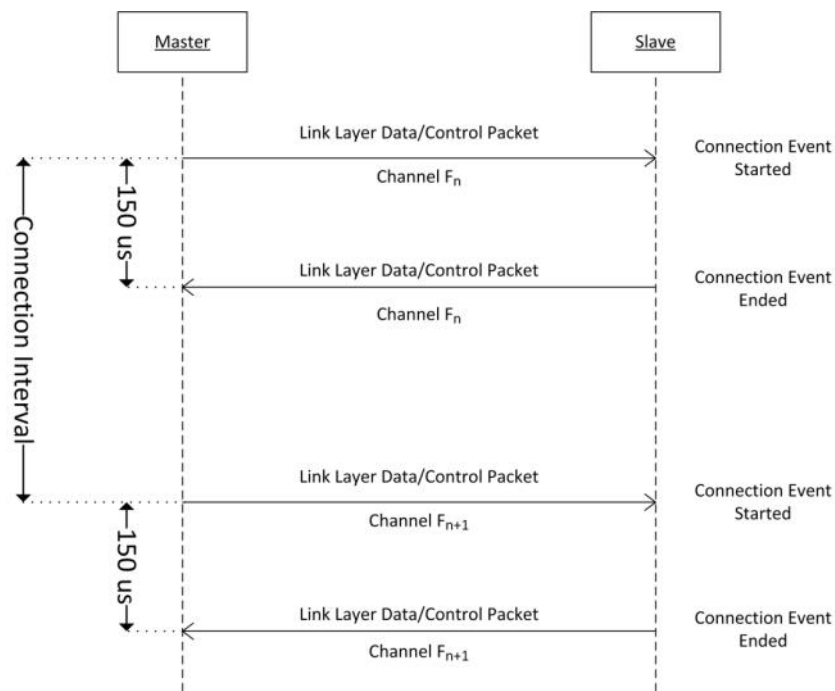


**Figure 18: BLE connection interval** [44]

Connection event happens when two devices (sender and receiver) meets in a pseudorandom specific channel in the frequency-hopping scheme. As shown in Figure 18, the connection event is 150μs. Within each connection event, the slave is able to send 3 notification packets or 1 read/write request. The connection interval is the amount of time between two connection intervals. It is measured in units of 1.25ms and the smallest supported is 7.5ms. Smaller

connection interval will provide higher throughput at the cost of larger power dissipation. On the other hand, larger connection interval will dissipate lesser power but provide lower throughput. Note that even when there is no application data to be sent or received, two devices are obliged to exchange link layer data (synonymous to keep-alive or heartbeat messages) in order to maintain the connectivity.

Slave latency is a parameter which gives the slave device (ECG device) the option of skipping a certain number of connection events. This increases the flexibility and reduces power of the peripheral by longer sleep duration if it doesn't have any data to send. Therefore, reducing the slave latency will increase the power consumption but reduces the data transmission latency. Table 11 summarizes the features of 2 different microcontrollers, PIC18F46J50 and CC2540.

**Table 11: Comparison between various microcontrollers**

|  | **PIC18F46J50** [42] | **8051 on CC2540** [43] |
|---|---|---|
| SRAM | 3.69kB | 8kB |
| CPU Frequency | 12MHz | 32MHz |
| Wakeup Time | 1.5µs | 4µs |
| Hardware Serial Ports | 2 Serial (SPI/I$^2$C) | 2 Serial (SPI/UART) |
| UART Baud Rate | 921600 | 921600 |
| ADC | Yes | Yes |
| USB Support | Yes | Yes |
| Inbuilt Transceiver | No | Yes |

## 4.6    Conclusion

The major hardware components within in the wireless ECG device were described. This includes the power management integrated circuit for power regulation, ECG sensors for signal acquisition, transceivers for wireless communication, accelerometer for activity monitoring and microcontroller for overall system control.

# 5    Unified Software Platform for Wireless ECG System

## 5.1    MCU Firmware Design

The MCU firmware design of the wireless ECG device will be described by the use of sequence diagrams, state machine and design patterns.

### 5.1.1    Sequence Diagram

The UML sequence diagram of a typical interaction between the components in the ECG device is shown in Figure 19. The scenario highlights the involvement of an end-user (User) during the continuous transfer of ECG data that is acquired from the ECG device (consisting of Button, MCU, LED, Buzzer, Bluetooth and ECG Sensor) to the GUI (graphical user interface) of the client application. It also includes the interactions used to update the ECG configuration such as the ECG gain. In the case of CC2540 SoC (integrated MCU and the Bluetooth transceiver), the MCU and Bluetooth module on Figure 19 can be treated as a single entity.
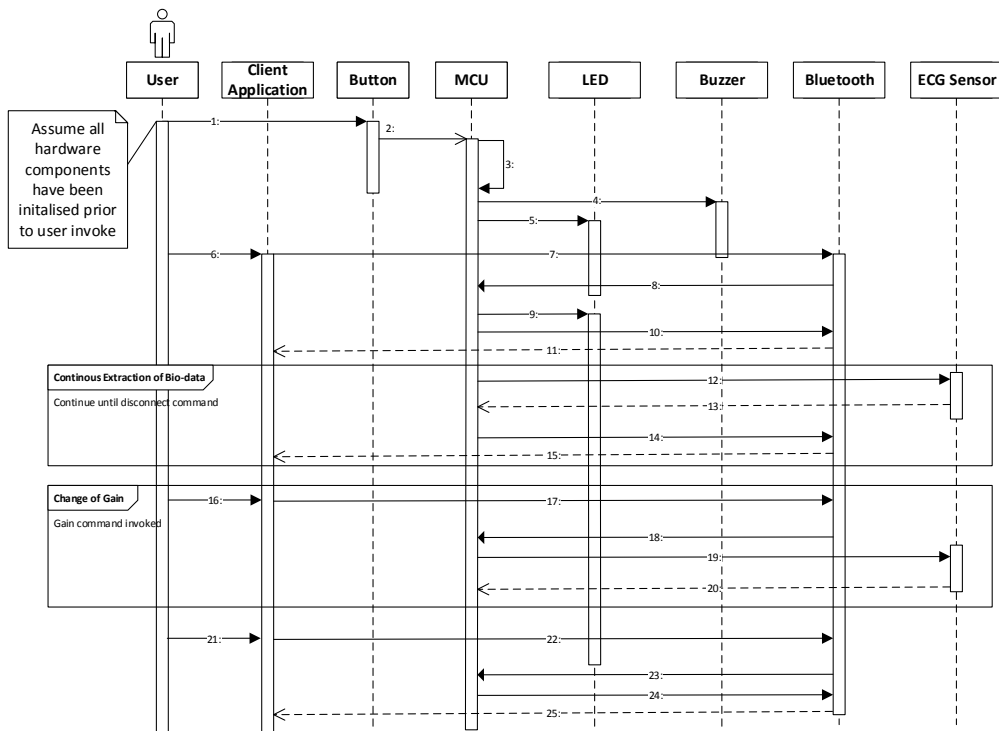
**Figure 19: Sequence diagram of a general startup of an ECG sensor**

Prior to the start of the sequence on Figure 19, the hardware components are assumed to have been initialized. The numbered sequences are explained as follows:

1: The User pushes the button.

2: The Button signals an interrupt to the MCU.

3: The MCU registers the interrupt and check if it is held for more than X seconds.

Step 2 and 3 is used to startup the ECG device from sleep mode. It can be co-designed on hardware whereby the LTC3553 chip will check if X seconds has surpassed.

4: The MCU generates a signal pattern to the buzzer to beep.

5: The MCU generates a pattern on the LED indicating the standby state.

6: The User invokes Connect command via the GUI of the client application.

51

7: The Connect command is sent to the Bluetooth module as invoked via the GUI of the client application.

8: The Bluetooth module relays the Connect command to the MCU.

9: The MCU generates a pattern on the LED indicating the connect state.

10: The MCU generates an acknowledgement message and sends it to the Bluetooth Module.

11: The Bluetooth module relays the acknowledgement to the client application.

12: Once the ECG Device is in the Connect state, there is an implicit interrupt from the ECG Sensor to indicate that data is ready. The data transfer signal is initiated by the MCU via the SPI protocol.

13: The ECG sensor returns the raw ECG data to the MCU via the SPI protocol.

14: The said ECG data is packetized and then sent to the Bluetooth module.

15: The said ECG data is sent to the client application. Item 12 to 15 repeats until Disconnect command is invoked.

16: In the mean-time, the MCU can invoke a Gain update command onto the ECG sensor. The User invokes the Gain command via the GUI of the client application.

17:  The Gain command is sent to the Bluetooth module.

18: The Bluetooth module relays the Gain command to the MCU.

19: The MCU invokes a gain update during the process of ECG data query.

20: The MCU receives the Gain command acknowledgement from the ECG sensor.

21: The User selects the Disconnect GUI on the client application.

22: The Disconnect GUI is converted into commands and sent to the Bluetooth module.

23: The Bluetooth module relays the Disconnect command to the MCU.

24: The MCU receives the Disconnect command and changes its state. Then, the MCU sends an Acknowledgement command to the Bluetooth module.

25: The Bluetooth module relays the Acknowledgement command to the client application.

## 5.1.2    System Firmware State Machine
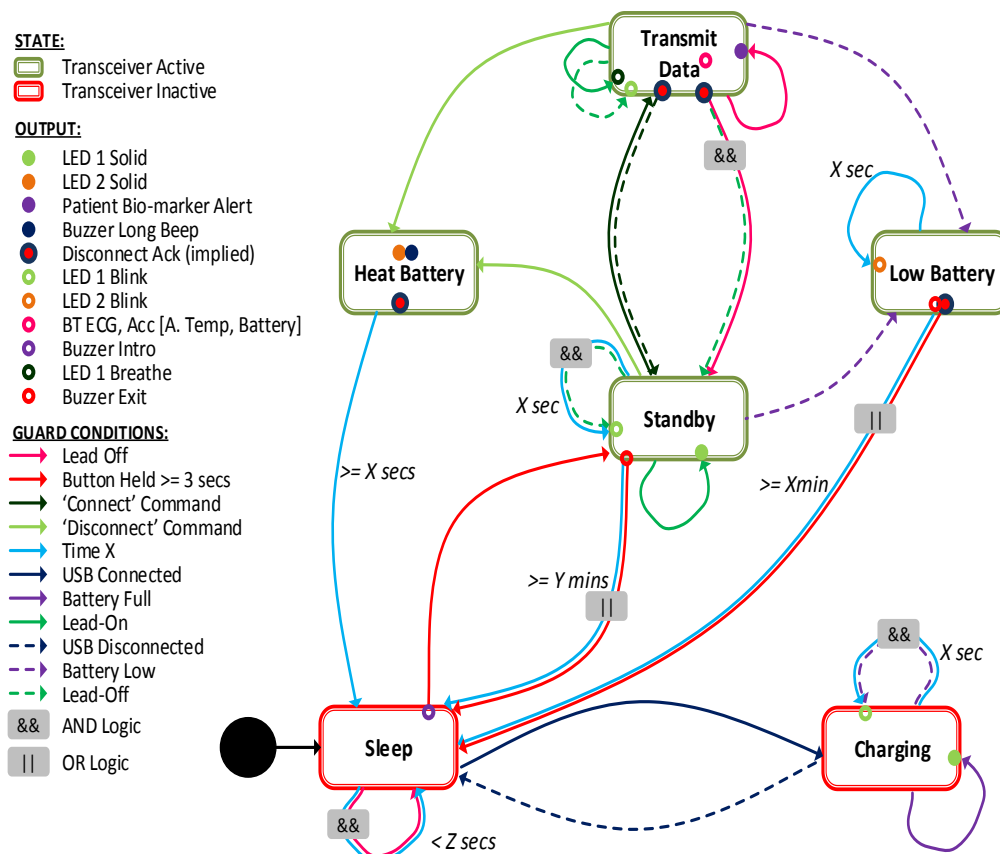


**Figure 20: System-level state diagram**

The system firmware state machine covers the steps involved in the use case as of Figure 7. There are 6 states and the colour surrounding each state represents the transceiver status – active (green) or inactive (red). Active

53

means that the transceiver is drawing power to perform activities such as discovery and transmitting data whereas inactive means that the transceiver is disabled. The descriptions of the 6 states are as follows:

Sleep: The device goes from the Start state to the Sleep state automatically when the battery is connected. The Sleep state consumes the lowest power. In this mode, all peripherals including the Bluetooth are disabled. The static power dissipation is dominant in this state. The MCU is programmed to wake up only when the button on the ECG device is pushed. Optionally, the transition to the Standby state is followed by a buzzer entry tone.

Standby: In the Standby state, the ECG device listens for the Connect command from the client application and once received, it will transit into the Transmit Data state. In this state, the ECG device will blink if the electrodes of the device are not in contact with the human skin (lead-off). The LED will stop blinking when the electrodes of the ECG sensor are in contract with the skin.

Transmit Data: In this state, the MCU extracts the ECG data from the sensor and then transmit it to the client application. The additional sensor data acquired may include bio-impedance for respiratory rate, temperature, accelerometer, etc. This is the most power consuming mode. A portion of the power consumption is contributed by the transmitter and the execution of the protocol stack. Therefore, reducing the amount of data transmitted through compression can significantly reduce the overall power consumption. Section

6.3.3 contains the profiling of the battery discharge plot during continuous transmission. In addition to the continuous transmission, the ECG data may also be recorded on the client application. This state also models the user pressing the button to send an event marker if he feels uncomfortable. In the Transmit Data mode, the LED can breathe to indicate normal operation or lead-on. Otherwise, the LED will blink. The Transmit Data state will transit into the Standby state happens when Disconnect command is received or when lead-off happens and the button is pressed.

Charging: In Charging Mode, the ECG device's in-built battery is charged via a USB port. When the device is fully charged, the LED will stop blinking and turn solid. Upon USB removal, the device will return to Sleep mode.

Low Battery: The device transits into the Low Battery state whenever the battery life falls below a certain voltage threshold. This applies to all states except for the Standby, Charging and Heat Battery state. Upon entering the Low Battery state, all prior operations are suspended. In the Low Battery state, the LED will blink for X seconds and exit gracefully into the Sleep state. Optionally, the transition to the Sleep state is embedded with a buzzer exit tone.

Heat Battery: The Heat Battery state is designed as a safety feature within the ECG device. If the temperature of the battery in device reaches above $50^{\circ}$C, Heat Battery state will be triggered from various operational states except for the Sleep state. In this mode, all prior operations such as data transmission are

55

halted and the ECG device goes back to Sleep state. Optionally, the buzzer can produce a long beep to alarm the user and the LEDs may turn solid.

### 5.1.3 Design Patterns

A real-time design pattern for embedded systems is used to generalize certain type of functions that can be customized for different embedded applications. There are different types of commonly used design patterns in the MCU's firmware.

Static factory pattern ensures that only a single instance is initiated at the entire course of the program; in this case, a single circular buffer for the Bluetooth receiver buffer as shown in Figure 21. Composition means that the callee came to existence because of the call from the main class (caller). Via a singleton programming keyword, the ConcreteCircularBufferFactory ensures that the initialization happens only once as also shown via the 1 to 1 relationship between the main class and the ConcreteCircularBufferFactory [45]. The memory allocated is assigned to a high priority circular buffer for receiving asynchronous incoming data via the MCU's interrupt.
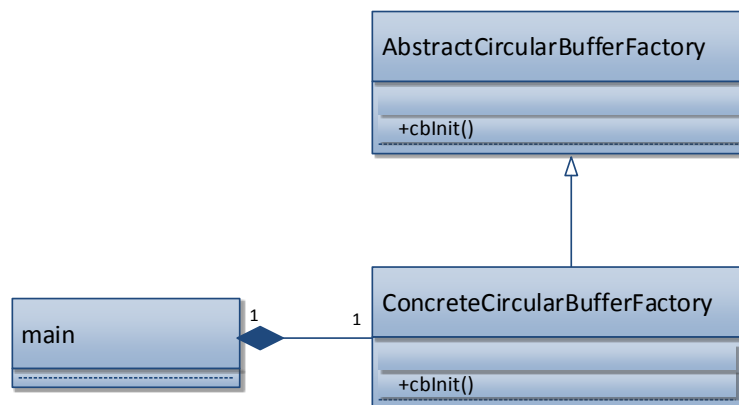


**Figure 21: Static factory design pattern for Bluetooth receiver buffer**

The UML class diagram of the round-robin scheduler with interrupt is illustrated in Figure 22 [46] [47]. The scheduler is an event driven model. There are four component classes namely, Scheduler, Event Interrupt, Abstract Task and Concrete Task. There is a single Scheduler which will receive various interrupts from the Event Interrupt class. This interrupt can come from sensor acquisition, button pressed, timer interrupt, etc. The scheduler will invoke the concrete task via a function pointer through an orderly task list.
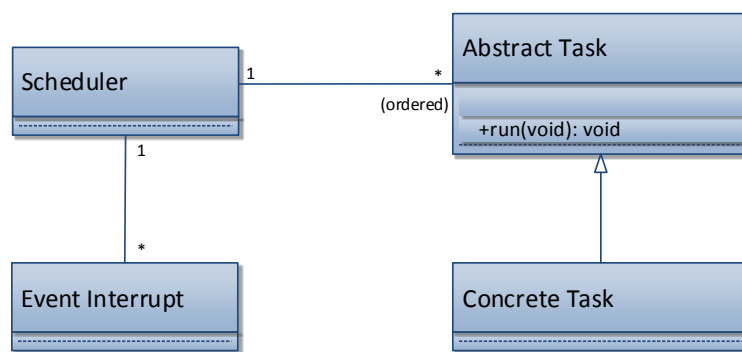


**Figure 22: Round-robin scheduler with interrupt design pattern**

The round-robin scheduler with interrupt can be combined with the dynamic frequency scaling to reduce dynamic power whereby the MCU will scale its frequency based on the task workload as generated through the event interrupt. The pattern is also able to allow the MCU to stay in idle mode (power saving) and then switch to active mode upon receiving event interrupts.

## 5.2    Client Application

The client application is also known as a personal gateway. It is used to display the signals that are acquired and transmitted from the ECG device via the Bluetooth protocol. These signals in their raw form possesses less

meaningful information and must be computationally filtered or transformed into a more meaningful form.

### 5.2.1 Removing Baseline Drift using High Pass Filter

ECG Baseline drift is an ECG artifact or noise whereby the baseline of the ECG is not flat but rises and falls with time as shown in Figure 24. Both NUS Chip (with buffer mode or data compression) and the commercial ADS1292R suffers from the baseline drift [27] [38] [27].
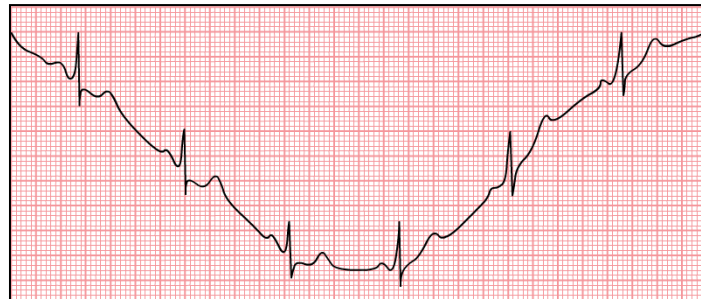


**Figure 23: Example of baseline drift on an ECG signal** [48]

For GUI ECG display and heart rate RR derivation, the baseline drift is removed by introducing a high pass filter as shown in Equation $5 - 1$.

$$Baseline\ Drift\ Correction(n) = x(n) - \frac{\sum_{i=n-k+1}^{n} x(i)}{k} \quad (5-1)$$

Whereby:

k is the number of samples at 256.

n is the current index.

x is the sample.

After the filtering, the Baseline Drift Correction(n) through the filter is plotted instead of its raw form x(n).

### 5.2.2 Activity Index

The activity index is a measure of movements or activity using the proper acceleration or g-force from the axis of a 3-dimensional accelerometer. In other words, instead of displaying the X, Y and Z g-force of the accelerometer, the X, Y, Z are translated or correlated into an activity index. For example, activity index can range from 0 to 100. Activity index of 0 to 32 signifies that the end-user is 'relaxed'. Index of 33 to 65 implies that the end-user has done 'moderate' activity and 66 and above implies 'intensive' activity. Activity index is useful as it can correlate to the ECG signals such as the heart rate. For example, high activity index with a fast heart rate is normal.

The activity index is a heuristic measure and is derived using the leaky integrator filter as shown below:

$$y[n] = \tau y[n-1] + (1-\tau)x[n] \qquad (5-2)$$

Whereby:

$\tau$ is a real number ranging from 0 to 1.

y is the local average.

The objective of the first term prior to the addition is to keep only a fraction of $\tau$ of the accumulated value and forget or leak a fraction of 1-τ. The objective of the second term after the addition is to add only a fraction of 1-τ of the current value to the accumulator. In addition, the filter is recursive since it uses its previous output value (feedback value).

Equation 5 – 3 is invoked to obtain the moving average of variable

gravity(x) with weights focusing on the accumulator.

$$gravity(x) = alp * gravity(x) + (1 - alp) * AAxis(x) \quad (5 - 3)$$

Whereby:

x refers to an index of an axis of a 3-dimensional accelerometer. Eg. X, Y or Z

plane.

alp refers to the alpha filter coefficient strength at 0.8.

AAxis refers to the magnitude of the accelerometer's axis.

Following that, a high-pass filter is invoked to subtract the current sample,

AAxis(x), from the average gravity as shown in Equation 5 – 4.

$$AAxis(x) = AAxis(x) - gravity(x) \quad (5 - 4)$$

The magnitude from Equation 5 – 4 is then obtained as shown in Equation 5 –

5.

$$AM = \sqrt{\sum_{x=1}^{y} (AAxis(x))^2} \quad (5 - 5)$$

Whereby:

y refers to the total number of axis in a 3-dimensional accelerometer. In this

case, y is 3 for a 3-d accelerometer.

AM is the accelerometer magnitude.

For tuning purposes, the moving average based on leaky filter is focused on

the accumulator as shown in Equation 5 – 6.

$$MS = beta * MS + (1 - beta) * AM * gain \quad (5 - 6)$$

Whereby:

AM is the accelerometer magnitude.

MS is the filtered accelerometer magnitude or activity index.

beta refers to the accumulated strength at 0.995

gain refers to amplification to the magnitude smoothened at 2.5 (heuristics).

The multiplication with gain will increase the rate of change of MS.

### 5.2.3 Heart Rate

The heart rate refers to the speed of the heart beat which is usually expressed in beats per minute (bpm). The client application will receive the raw ECG signal and the heart rate can be derived using the process flow as shown in Figure 24. The heart rate detection uses the leaky integrator filter as a means to detect the R peak. This method is done qualitatively on heuristics and has been simulated in Matlab. It is also implemented on a client application device such as PC and smartphone application for real-time RR detection.
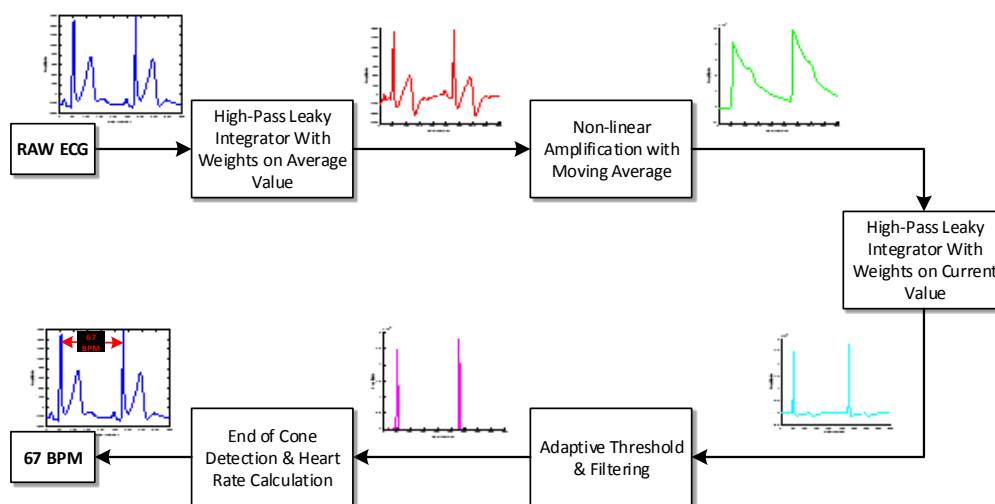


**Figure 24: Overall process to calculate the heart rate using the ECG signals**

'High-Pass Leaky Integrator With Weights on Average Value' focuses on smoothing the signal by averaging. This filter will also reduce the amplitude of the low frequency signal. In other words, the amplitude of the T-wave will fall around the baseline.

The 'Non-linear Amplification with moving Average' first performs a cube on the current value and subtracting against the previous accumulated value before suppressing the value into the accumulator. The suppressor (division operation) at 100 allows the wave to fall smoothly.

'High-Pass Leaky Integrator With Weights on Current Value' is a leaky high-pass filter that emphasizes weights on the current value. This filtering results to very distinctive spikes. 'Adaptive Threshold And Filtering' is used to dynamically update the threshold and removes any values below the threshold leaving only a spike as shown in Figure 24.

'End of Cone Detection & Heart Rate Calculation' uses a lock and unlock mechanism to detect or lock the start of a cone (values greater than threshold as done in previous step) and unlock at the end of cone (values lesser than threshold as done in previous step). There is also a false positive check by measuring the width of the cone.

$$HeartRate = \frac{256}{RR\ Interval} * 60 \qquad (5-7)$$

The heart rate calculation can be calculated by obtaining the number of samples between two RR intervals (R to R peaks in the ECG signal) as shown in Equation 5 – 7:

### 5.2.4   Alerts: Lead-off and Marker

During data acquisition, the client application receives alerts from the AFE via the ECG device when the contact of the electrodes is not good. In addition, lead-off alerts will be masked when the contact is good. In moments where the user feels uncomfortable, a marker can be tagged into the data captured. These features are done in accordance to the firmware state machine.

### 5.2.5   PC Application
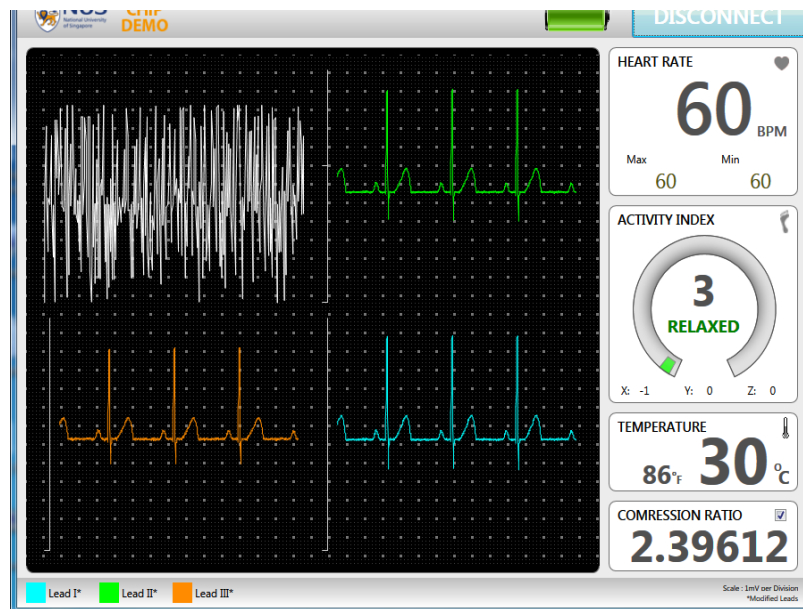


**Figure 25: PC (Windows) application**

Figure 25 shows a Windows PC application to view the leads and activities of the ECG device in real-time. The application is written on Microsoft Visual Basic. The compressed signal is shown on the top-left corner of the plot. The

blue, green and orange plot represents the Lead I*, Lead II* and Lead III* respectively. Symbol '*' means that they are non-standard leads placement.

The battery life is shown beside the Disconnect button. Below the Disconnect button shows the real-time heart rate followed by the activity index, temperature in $^o$C and $^o$F and the compression ratio. The minimum and maximum heart rates are also displayed in the Heart Rate pane. For a single-lead device operation, only a single-ECG lead will appear on the plot and the rest of the leads will be masked out.

### 5.2.6    Smartphone Application
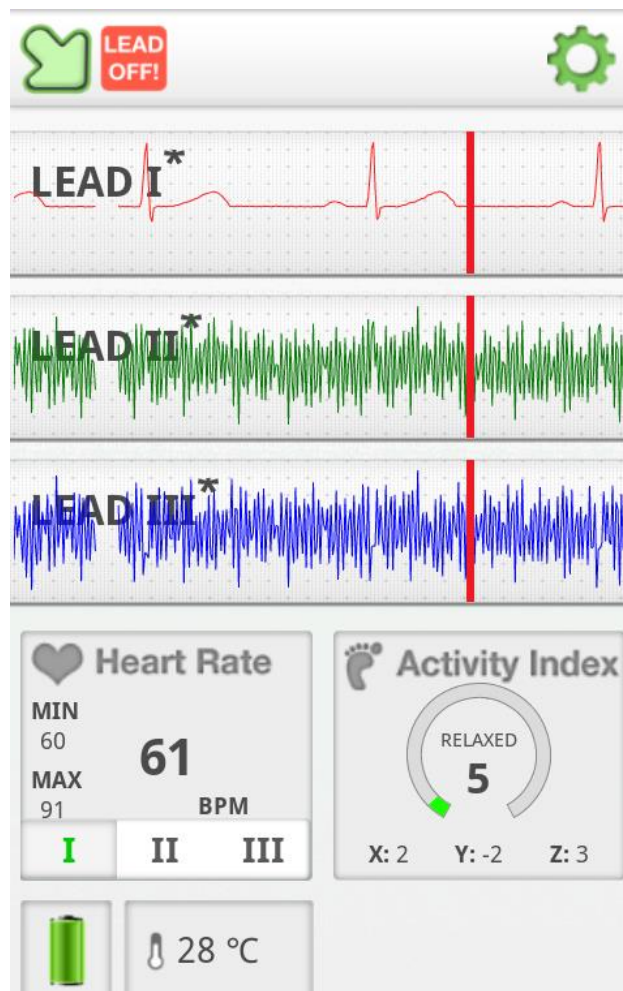


**Figure 26: Mobile application**

The client application on a smartphone for the ECG device is illustrated in Figure 26. It is programmed in the Java programming language and executed on the Android Dalvik Java Virtual Machine platform. The features are similar to the PC application except that the layout has been re-arranged in a portrait orientation. Figure 26 shows a scenario where the LL (Left Leg) electrode is intentionally detached from the body. As a result, the lead-off error appears on the top-left corner. At the same time, the user pushes the button on the ECG device and an alert (vertical red) appears on all ECG leads. Since the ECG data can be streamed onto the smartphone, the data can also be recorded. For a single-lead device operation, only a single-ECG lead will appear on the plot and the rest of the leads will be masked out.

## 5.3    Conclusion

The design of the unified software platform for wireless ECG system was introduced. The UML diagrams such as sequence diagram are used to describe the firmware design. This is followed by an internal state machine of the ECG device and certain design patterns to characterize the common handling mechanisms within the firmware. On the client application, certain features such as baseline drift, activity index from the accelerometer, alerts during lead off and markers were developed on the PC application and smartphone.

# 6 Power Optimization Using Co-Design Techniques

The main objective of Section 6 is to discuss on the limitation of the power optimization techniques on the CB ECG device which leads to the design considerations and power optimizations for the low-power BLE ECG device.

## 6.1 Classic Bluetooth ECG Device

The hardware of the single-lead Classic Bluetooth ECG (CB ECG) device was pre-designed [5]. It has a PIC18F46J50 MCU for overall system control, WT-12 Classic Bluetooth module for ECG data transmission, MT29F16G08 NAND flash for on-device storage, NUS ECG Chip with Buffer Mode for ECG signal acquisition and LDO for power regulation.



**Figure 27: Prototype of the Classic Bluetooth ECG sensor**

The WT-12 transceiver module acts as a bridge for sending and receiving data for the microcontroller. The bridge configuration enables more choices of microcontroller since most microcontrollers have the UART interface. This gives the hardware designer the flexibility to choose a high pin count microcontroller or lower pin count with IO peripheral support (SPI, $I^2C$) depending on the components that are to be connected. The throughput provided by the Classic Bluetooth module is capable of supporting up to 12-

lead ECG transmission. However, this design comes at a cost of high power dissipation during continuous transmission. The system power profile without optimization has been discussed in Section 2.1.2. The supply voltage of the device is held at 3.28V and the total current dissipated is 42.06mA. Classic Bluetooth module consumes about 52.9% and the MCU at 35.4% which sum up to 88.3% of the total power dissipated.

### 6.1.1 Optimized Continuous Streaming

In this configuration, the wireless ECG device transmits real-time ECG data continuously with power optimization on the MCU and on-device flash. The components that supports sleep mode and fast wake up time, such as the flash storage, toggles between the active/idle modes during write in order to reduce dynamic power consumption. The optimization technique leverages on the design pattern of the round-robin scheduler with interrupt on the MCU whereby interrupted tasks are handled by increasing the clock frequency and upon task completion, the frequency is reduced. The streaming latency of the ECG data from the ECG device remains identical as the non-optimized during the continuous transmission because data are transmitted immediately after each interrupt (generated by the ECG sensor).

The power optimization on the Classic Bluetooth module was not possible because the module is continuously and actively waiting for new inputs from the external MCU. It will automatically go to idle mode (sleep) after at least 1 second of inactivity. It was observed that the power consumed during the active mode is about the same. This is mostly because the Classic Bluetooth

module is embedded with a pre-configured BlueCore 4 microcontroller and a radio transceiver which will only go into the idle mode after 1 second of inactivity. Therefore, this means that it is not possible to switch between active/idle modes in order to reduce power consumption given the real-time requirements (R.M.1.1) to transmitting the ECG data.
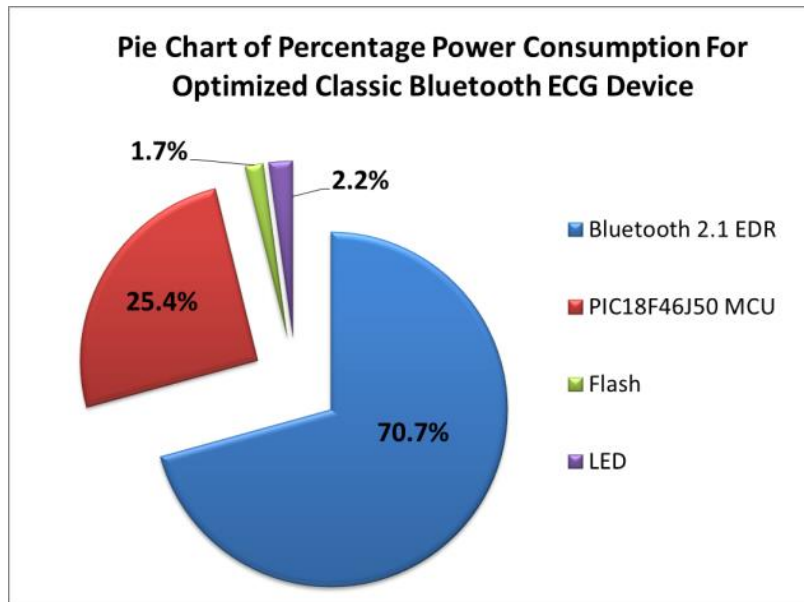


**Figure 28: Pie chart of power consumption for optimized Classic Bluetooth ECG device**

Figure 28 depicts the pie chart of the power consumption of various components in an optimized high-data rate ECG device. The power breakdown is tabulated in Table 12. The supply voltage of the device is held at 3.28V and the total current dissipated is 31.47mA. It can be seen that the Bluetooth 2.1 EDR (Classic Bluetooth) module consumes the most amount of energy at 22.26mA followed by the MCU, which is reduced from 14.89mA to 8mA. The total power dissipated by the Classic Bluetooth and the MCU sums up to 96.1%. After optimization, the flash memory takes up about 0.53mA and the LED remains at about 0.68mA.

**Table 12: Tabulated power breakdown for optimized Classic Bluetooth ECG device**

|  | Current (mA) | Percentage |
|---|---|---|
| Bluetooth 2.1 EDR | 22.26 | 70.7% |
| PIC18F46J50 MCU | 8.00 | 25.4% |
| Flash | 0.53 | 1.7% |
| LED | 0.68 | 2.2% |
| Total | 31.47 | 100% |

### 6.1.2   Summary

The design and power optimization techniques for the CB ECG device, with recording capabilities were described. It is noted that the Classic Bluetooth module is able to support continuous ECG streaming of up to 12-lead. However, the power consumed of the CB ECG device after optimization is still high, around 99.25mW (3.28V by 30.26mA). The power breakdown shows that the power hotspot lies at the transceiver and the MCU which constitutes about 96.1% of the total power. A low-power ECG device will be introduced to reduce the overall power consumption given the same constrains of supporting a single-lead wireless ECG device.

## 6.2   Bluetooth Low Energy ECG Device

The general block diagram of a low-power Bluetooth Low Energy (BLE) ECG device is depicted in Figure 29. It uses an integrated SoC to substitute the MCU and transceiver block into single block called 'SoC MCU with Bluetooth' to reduce power. The SoC has a BLE transceiver. The MCU has digital I/O and peripheral interfaces for inter-chip communication such as SPI. The SPI interface is used to connect to the ECG sensor. In this design, the SoC

has to handle the workload (BLE stack) of the BLE transceiver. The peripheral support is dependent on the features and pin count supported by the SoC. This means that it is less flexible when compared against the module based as mentioned in Section 6.1. For example, if hardware $I^2C$ is not supported, it can be emulated by the digital I/O via firmware provided that there are pins available.
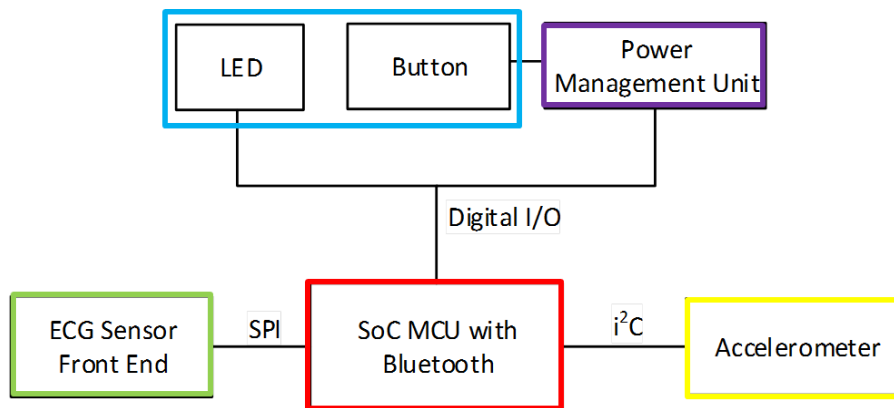


**Figure 29: Block diagram of a low-power BLE ECG device**

Furthermore, the button is connected to the 'Power Management Unit' block and then relayed to the SoC. The 'Power Management Unit' block has an internal state machine designed for minimizing static power dissipation when the ECG device is not in use.

### 6.2.1 Module to SoC

The motivation of using the SoC is mainly due to the profiling results of the CB ECG device showing that more than 90% of the power consumption originates from the MCU and transceiver during ECG transmission. Thus, the goal of the SoC is to reduce the power dissipation by means of using an

integrated system (SoC CC2540) with a low-power transceiver to enable longer hours of continuous transmission.
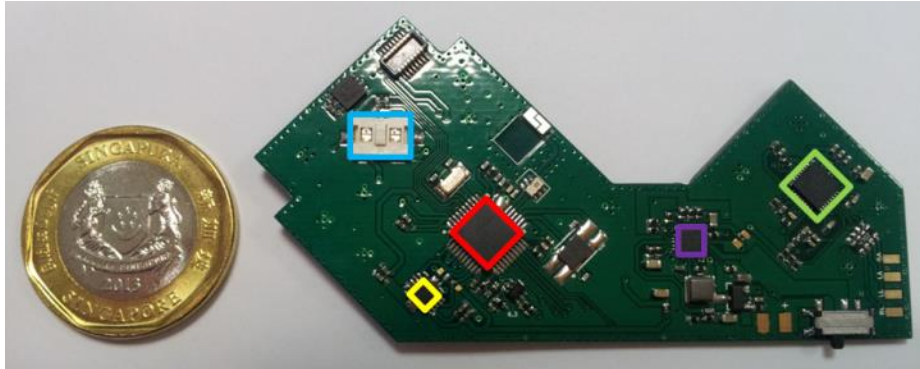


**Figure 30: The PCB of a low-power BLE ECG device**

The blocks of Figure 29 are mapped and color coded to the hardware implementation as shown in Figure 30. Figure 30 shows the PCB of a low-power BLE ECG device capable of transmitting a single-lead ECG and a single bio-impedance channel. The device uses an integrated SoC (TI CC2540 (red) as mentioned in Section 4.5.2). The integrated SoC contains a microcontroller and a BLE (Bluetooth 4.0) transceiver for controlling the firmware application and running the BLE stack.

The ADS1292R (green) is chosen as the AFE or the ECG sensor [38]. It can perform ECG and bio-impedance measurements. The LTC3553 (purple) is used as the power management unit. More details on the design will be discussed in Section 6.2.3. The MMA8452Q (yellow) is the accelerometer for generating the activity index. The button and LED (blue) comes as a single integrated component.
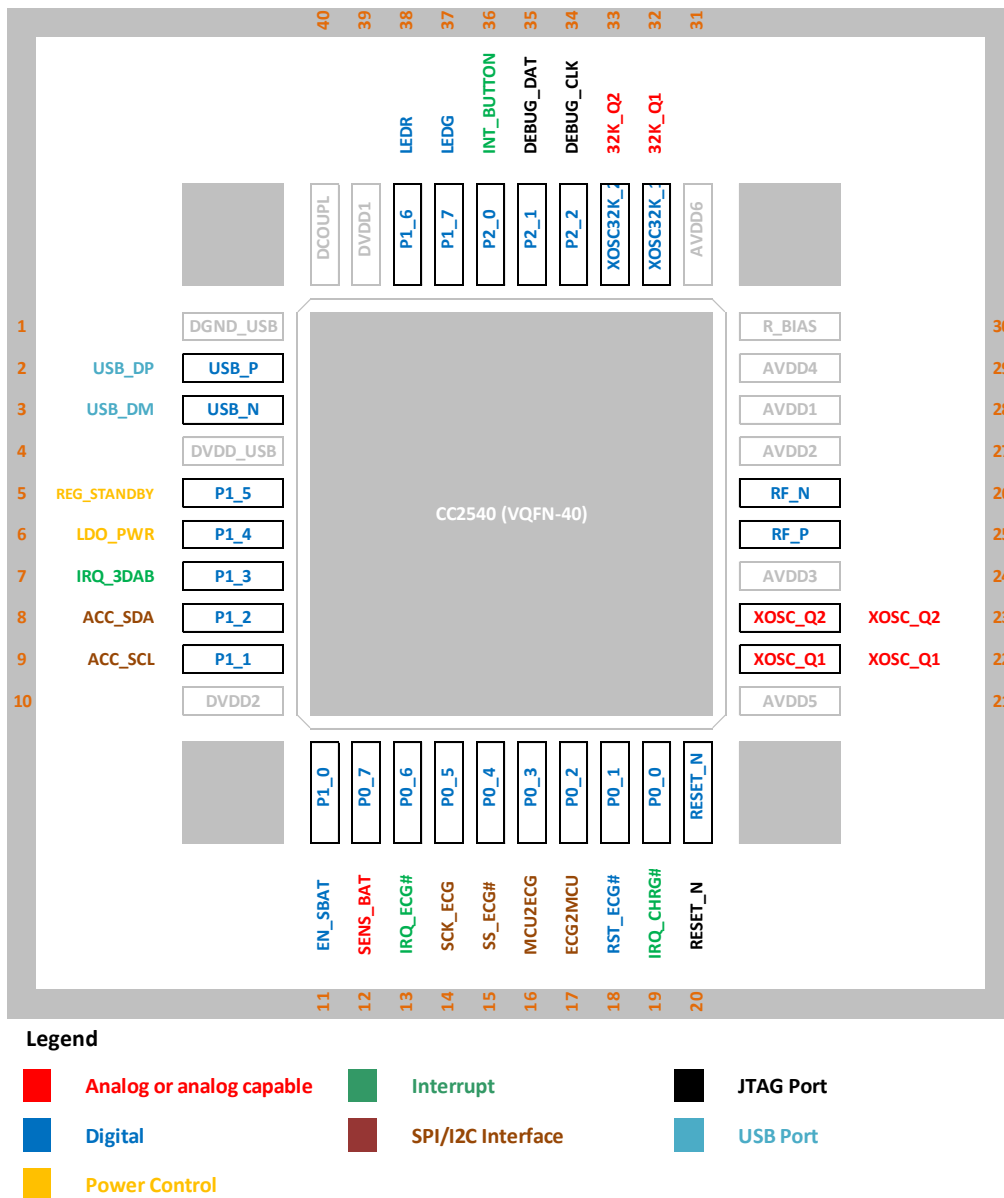
**Figure 31: CC2540 SoC pin mappings**

Figure 31 shows a CC2540 SoC on a VQFN-40 package. The schematics that follow the pin mappings for Figure 31 (CC2540 SoC) are shown in Appendix A. The pins are numbered in an anti-clockwise direction starting from the top left DGND_USB. The pins are colour coded whereby red represents the analog or analogue capable pins, dark blue for digital pins, gold for power control, green for interrupt, brown for peripherals, black for JTAG programming and light blue for USB ports.

The power management unit and LED are controlled by the SoC via power control and digital I/O pins. The button is connected to the power management unit and will trigger a filtered (de-bounced) signal from the power management unit to the pin 36 of the SoC [37]. The $I^2C$ interface is used to communicate between the SoC and the accelerometer via pin 8 and 9. The SPI interface is used to communicate with the analog front-end (AFE) sensor via pin 14 to 17.

The CC2540 SoC requires an antenna for ECG transmission. The PCB layout for the chip antenna design for transceivers at 2.4MHz plays a crucial role towards the power consumption of the device. Higher loss antenna design means that there are higher chances of bit error leading to more re-transmission by the baseband. It also affects the functional requirements (correctness) during data transmission.

The CC2540 has an output differential impedance of 70 + j30 ohms. However, the chip antenna requires an impedance of 50 ohm. The chip antenna is preferred over PCB antenna because chip antenna requires lesser board space. For maximum power transfer to happen, both the impedance must match and a balun is inserted for this purpose. In addition, the balun also converts the differential output of the CC2540 into the single ended output for the chip antenna.

During PCB design, the trace width between the balun and the chip antenna has to be matched at 50Ω. The general formula of the calculated impedance on the PCB is given by Equation 6 – 1.

$$CI = \frac{87}{\sqrt{Er + 1.41}} * ln\left(\frac{5.98 * TTPD}{0.8 * TW + TH}\right) \qquad (6-1)$$

Whereby:

TTPD is the 'trace to plane distance' at 11.81mil.

TH is the 'trace height' at 0.04mil.

CI is the 'calculated impedance' at 50Ω.

Er is the dielectric constant or relative permittivity of FR-4 at 4.3.

TW is the trace width.

Rewriting Equation 6 – 1,

$$TW = \left(\frac{5.98 * TTPD * 87}{e^{CI \times \sqrt{Er + 1.41}}} - TH\right) * 1.25 \qquad (6-2)$$

Using Equation 6 – 2, the trace width (teal) is found to be 20.68mil as drawn in Figure 32
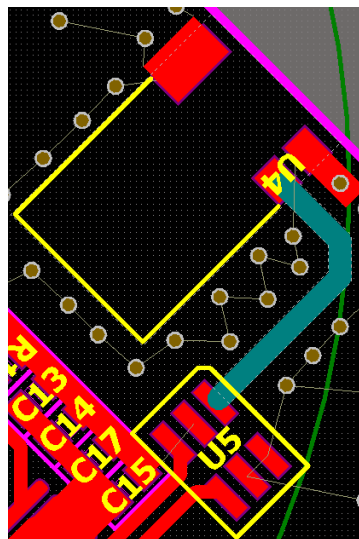


**Figure 32: Trace width between balun (U5) and chip antenna (U4)**

As described in Section 4.5.2, the connection interval and slave latency will affect the power consumption. Table 13 tabulates the BLE settings used in the power profiling on Table 14. The connection interval is configured to 7.5ms. This is the smallest value that can be accepted by the BLE stack. The second configuration, the slave latency is also configured to 0 which means that no connection events can be skipped.

Table 13: Bluetooth Low Energy SoC transmission settings on CC2540

| Settings | Time (ms) |
|---|---|
| Connection Interval | 7.5 |
| Slave Latency | 0 |

The configurations stated in the previous paragraph are the most power consuming settings but provides the highest throughput in order to satisfy the continuous transmission of the ECG stream in the ECG device. It is also experimentally observed that it provides the most reliable transmission for continuous transmission.

Following the experiment in the previous paragraph, it is known that the most power consuming settings allows reliable transmission. In the next experiment, the most power consuming settings is maintained and the transmission rate is gradually increased as shown in Table 14. The objective is to find the maximum transmission rate that can be supported during continuous transmission. Throughout the experiment, the voltage is held at about 4.05v. The Paired (mA) field refers to the current consumed after the BLE pairing and prior to continuous data transmission. The current consumed by the ECG device ranges from 3.49mA to 3.53mA.

In Table 14, the Transmit Current (mA) field refers to the current drawn during continuous transmission. It is noted that the current consumption increases as the frequency of transmission increases.

**Table 14: Profiling power consumption based on different data transmission rate**

| Transmit Rate (Hz) | Voltage (v) | Paired (mA) | Transmit Current (mA) | Missing Frame? |
|---|---|---|---|---|
| 31.25 | 4.05 | 3.53 | 4.57 | None |
| 62.5 | 4.05 | 3.51 | 4.87 | None |
| 125 | 4.05 | 3.48 | 5.77 | None |
| 250 | 4.05 | 3.49 | 7.18 | Yes |
| 512 | 4.05 | 3.53 | 8.75 | Yes |
| 1024 | 4.05 | 3.5 | 9.04 | Yes |

In Table 14, 'Missing Frame' field refers to whether the frame transmitted by the transmitter has been successfully received by the receiver. The 'Missing Frame' field is measured by padding a running sequence number at the BLE transmitter during ECG frame transmission. When a running sequence number is received at the receiver, this means that all frames have been successfully received and it is labeled as 'None' in the 'Missing Frame' field. However, in the event of a missing sequence number, this means that a frame was never received by the receiver and labeled as 'Yes'. It was experimentally observed that the missing frame and frame errors happens more often for frequency greater than or equals to 250Hz as shown in the 'Missing Frame' field of Table 14. This experiment is carried out within a period of 30 seconds.

Since the frequency of transmission is limited to 125Hz while the ECG sampling rate must be greater than equal to 250Hz as per requirement

R.M.1.3, two or more ECG samples can be packed together in a single 20-byte BLE notification frame.

It is also noted that the additional current drawn during continuous transmission is about 1.5mA for Transmit Freq of 125Hz. The current drawn is calculated by subtracting the Transmit Current (mA) against the Paired (mA) on Table 14. This shows that prior to continuous transmission (Transmit Current (mA)), the baseline current drawn after pairing (Paired (mA)) is already substantial (about 3.5mA). As described in Section 4.5.2, this is due to the execution of the MCU on the BLE stack, even when no application data is sent, in order to maintain the connection at link layer.

From Table 14, the rate of data transmitted by the SoC is a function to the power dissipated during transmission. Thus, this means that data compression can help to reduce the rate of transmission leading to lower power dissipation. This is known as fine-grained transmission. This ability is not available in module based Bluetooth transceivers such as WT-12 and KC-22 as used in the CB ECG device.

### 6.2.2  Lossless Data Compression

The objective of the lossless data compression is to further reduce the dynamic power dissipation during continuous ECG transmission. This is possible because lowering the transmission rate (due to lesser data after compression) can lower the power dissipation as shown in Table 14. This is

known as fine-grain transmission. With regards to the CC2540 SoC, the lossless compression algorithm is implemented within the 8051 MCU.

Figure 11 illustrates a block diagram of the data compression scheme (slope based compressor) as proposed in [27]. The ECG signal x(n) is pumped into the 'Slope Based Linear Predictor' and the output from the predictor is subtracted against the original signal forming the residue. The residue or e(n) is expected to be signal of low amplitude or energy. The residue is then fed into the 'Prediction Error Coding' block and 'Dynamic Fixed Length Packaging' block before sending to the client application. The purpose of these blocks is to repackage the residue into a fixed block as shown in Figure 34.
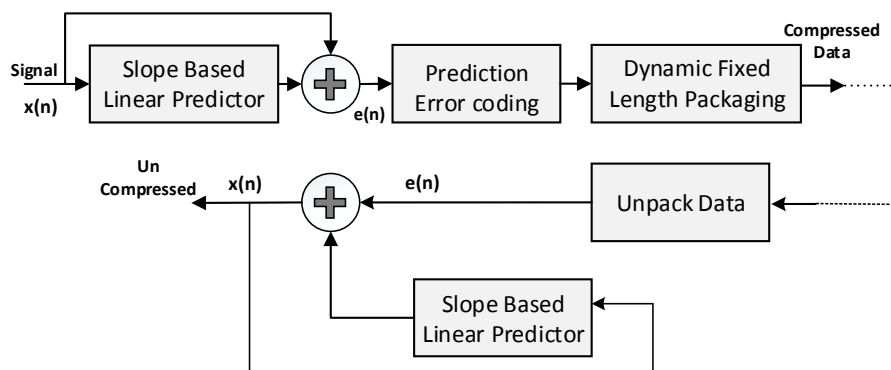


**Figure 33: General architecture of the slope based compression algorithm**

| Frame Type | Header | | | | Data | | | | | |
|---|---|---|---|---|---|---|---|---|---|---|
| **A** | 1 | | | | 5 bits | | 5 bits | | 5 bits | |
| **B** | 0 | 1 | | | 7 bits | | | 7 bits | | |
| **C** | 0 | 0 | 0 | 1 | 3 bits | 3 bits | 3 bits | | 3 bits | |
| **D** | 0 | 0 | 0 | 0 | 2 bits | 2 bit | 2 bits | 2 bits | 2 bits | 2 bits |
| **E** | 0 | 0 | 1 | 1 | 12 bits | | | | | |

← 16 bits →

**Figure 34: Data Packaging scheme for 2's coded prediction error symbols**

Figure 34 shows 5 types of compressed frame, Frame type A, B, C, D and E. A frame is defined as a single block of 16 bits. It consists of the Header and Data sub-frame. The Header sub-frame is used to identify the number of residual chunks within a frame. For example, Frame A contains 3 residual chunks with each chunk at 5 bits. In terms of compression ratio, Frame D has the highest compression ratio whereas Frame E has the least (using all 12 bits to store a single residue).

The details to the selection of packaging of each compressed frame (16 bits) are shown in Figure 35. Firstly, after collecting 6 residues from the 'Slope Based Linear Prediction' block, the selection is governed by checking the best fit starting from Frame Type format D, format C, format A, format B and finally format E. At the decompression stage, usually at the gateway, the reverse order is performed where the packaged data is unpacked using the 'Unpack Data' block. The 'Unpack Data' block produces sequences of residues, e(n), which is fed into and added with the inverse of the 'Slope Based Linear Predictor' to form the uncompressed data.

The lossless compression algorithm achieve an average compression ratio of about 2.25 when executed on the MIT-BIH Arrhythmia Database [27]. The algorithm is also known for its low-complexity requiring minimal hardware logics. During the firmware implementation of the algorithm into a SoC (CC2540), the slope based algorithm consumes about 0.44mW at 2.2V. As expected, the hardware compression consumes much lesser power at a mere 535nW at 2.4V [27]. During transmission, it is found that the current

consumption reduces by 1mA. The battery discharge plot of continuous ECG transmission with compression (SoC Transceiver Compression) can be seen in Section 6.3.3.
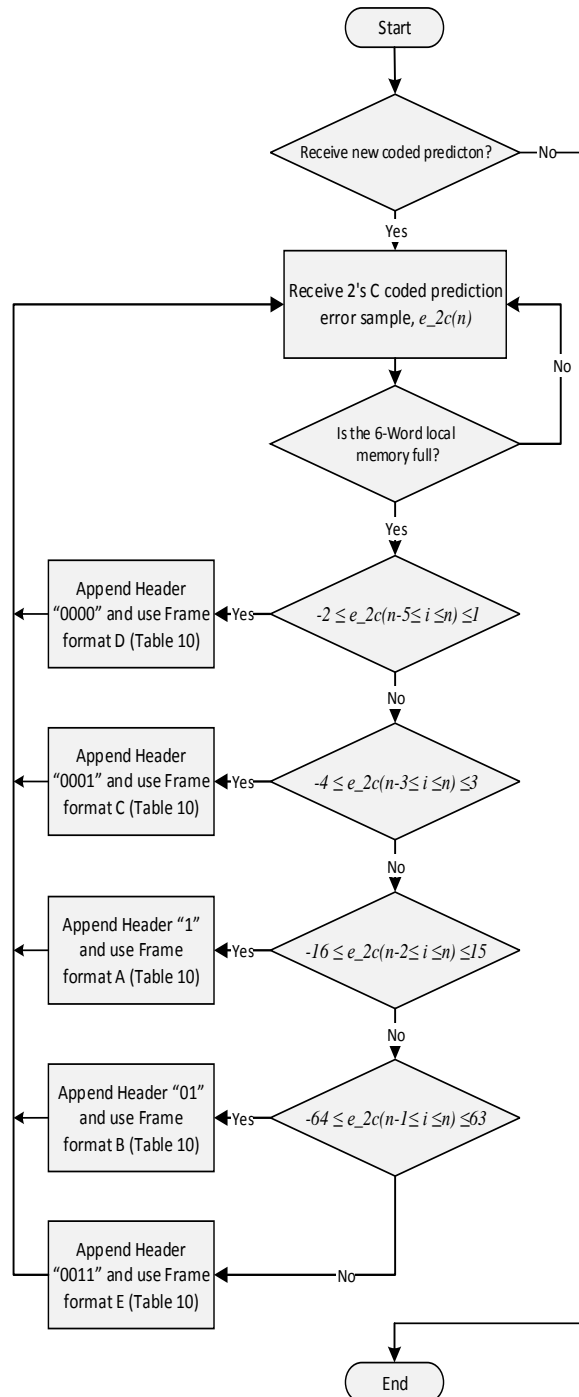


**Figure 35: Prediction error coding and selection of dynamic fixed length packaging**

### 6.2.3   Power Management on VLSI

The power management IC (LTC3353) is used to perform power management and optimization to reduce the dynamic and static power dissipation.
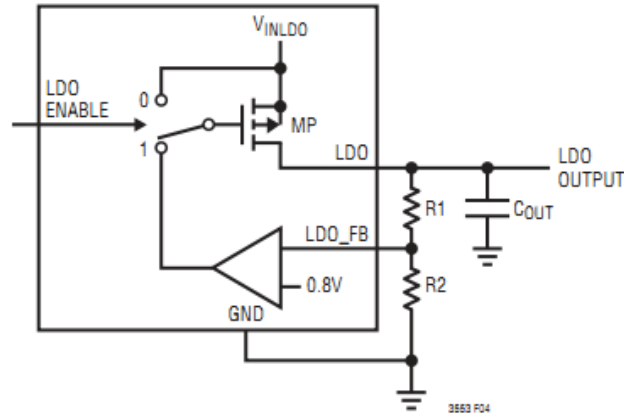


**Figure 36: LTC3553 LDO application circuit** [37]

The low dropout regulator (LDO) is a DC linear voltage regulator which regulates the voltage at 3.0V. The voltage supply is hardwired to the analog circuits of the AFE Chip. LDO is chosen because analog circuits such as the AFE require minimal noise for better acquisition accuracy [37].

$$V_{LDO} = 0.8\text{v} * \left( \frac{R1}{R2} + 1 \right) \qquad (6-3)$$

$$R1 = 1.54\text{M}\Omega \qquad (6-4)$$

$$V_{LDO} = 3.0\text{V} \qquad (6-5)$$

$$R2 = \frac{1.54}{\left[ \left( \frac{3.0}{0.8} \right) - 1 \right]} = 560k\Omega \qquad (6-6)$$

The output of LTC3553 $V_{LDO}$ is calculated based on the resistor ratio R1 and R2 as given in Equation $6-3$ [37]. R1 is shown in Equation $6-4$ and it is selectively chosen at 1.54MΩ. The voltage regulation $V_{LDO}$ required for the analog AFE is 3.0V as shown in Equation $6-5$. Rewriting, Equation $6-3$, we

81

have at R2 at 560kΩ as shown in Equation 6 – 6. The closest match commercial resistor is exactly matched to 560kΩ. Thus, R1 and R2 are set to 1.54MΩ and 560kΩ respectively in order to regulate $V_{LDO}$ at 3.0V.
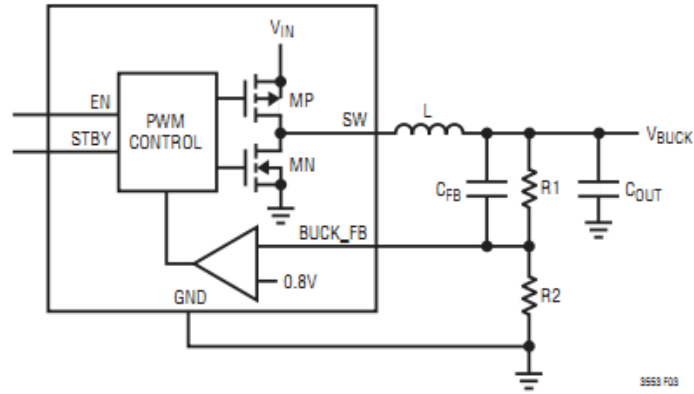


**Figure 37: LTC3553 buck regulator application circuit** [37]

The switch mode or buck regulator regulates the voltage by controlling the current in an inductor via a transistor and a diode. It is a more efficient means of regulation when compared against the LDO which uses heat dissipation for regulation. The voltage is regulated at 2.2V to the MCU/SoC, accelerometer and digital circuits of the AFE chip.

From the power profiling of the CB ECG device, it is noted that the transceiver and MCU can dissipate more than 90% of the total power. Therefore, reducing the voltage supply of the SoC is beneficial to reduce the power dissipation [16]. At the same time, the reduction of voltage supply to 2.2V has no impact on the clock frequency of the SoC [43]. The regulated voltage at 2.2V is also supplied to the digital portion of the AFE chip.

$$V_{BUCK} = 0.8v * \left(\frac{R1}{R2} + 1\right) \qquad (6-7)$$

$$R1 = 1.87\text{M}\Omega \qquad (6-8)$$

$$V_{BUCK} = 2.2\text{V} \qquad (6-9)$$

$$R2 = \frac{1.87}{\left[\left(\frac{2.2}{0.8}\right) - 1\right]} = 1.0686M\Omega \qquad (6-10)$$

$$R2 = 1.07M\Omega \qquad (6-11)$$

The switch mode voltage or $V_{BUCK}$ is obtained based on Equation $6-7$ [37]. Equation $6-10$ is a result of substituting Equation $6-8$ and Equation $6-9$ into Equation $6-7$. R2 is found to be 1.0686M$\Omega$. The closest commercial resistance available is valued at 1.07M$\Omega$ as shown in Equation $6-11$. Note that R1 is also selectively chosen at 1.87M$\Omega$ as it is commercially available. Plugging R1 and R2 back into Equation $6-7$, the voltage regulation is still at 2.20V when rounded to the nearest 2 decimal places.

Minimal battery discharge during sleep refers to the reduction of static power dissipation when the components in the ECG device are idle for a long period of time (eg. on the shelf) $-$ R.M.8.1. This is done by completely unpowering the voltage rails of the voltage regulator through similar methods as the power gating.

Figure 38 show the push button state machine of the LTC3553 Micropower USB Power Manager With Li-Ion Charger LDO Buck Regulator [37]. The state machine is mapped to two use cases:

1) Manual power down: The technical state machine can be mapped to a use case where the user holds the button for 400ms to turn on the device and holds for another 5 seconds to turn off the device: Upon

powering up with the Li-Ion battery for the first time, state PDN1 is activated via power-on-reset (POR). After 1 second, PDN1 transits to HR (hard reset). At HR mode, all power supplies are disabled and the internal power circuits are placed in an ultra-low quiescent state for minimal battery drain. The typical quiescent current at this state is about 0.2µA. The HR transits to the Power-On (PON) state when the button is held for more than 400ms. This completes the loop in green on Figure 38.

2) Automatic power down: On the other hand, if the user does not hold the button for 5 seconds and if the state machine of the ECG device is in the Standby state as of Figure 20, the ECG device can turn off automatically via a timer elapse. This is done by setting both BUCK_ON and LDO_ON (on Figure 31) to high via the MCU. When this happens, the PON state transits to Power Down 2 (PDN2). After 1 second, PDN2 will transit to Power Off (POFF). The typical quiescent current at this state is around 3µA.When the user holds the button for more than 400ms, the POFF state transits to Power Up 2 (PUP2) state and after 5 seconds, it goes into the active mode PON. This completes the loop in blue on Figure 38.
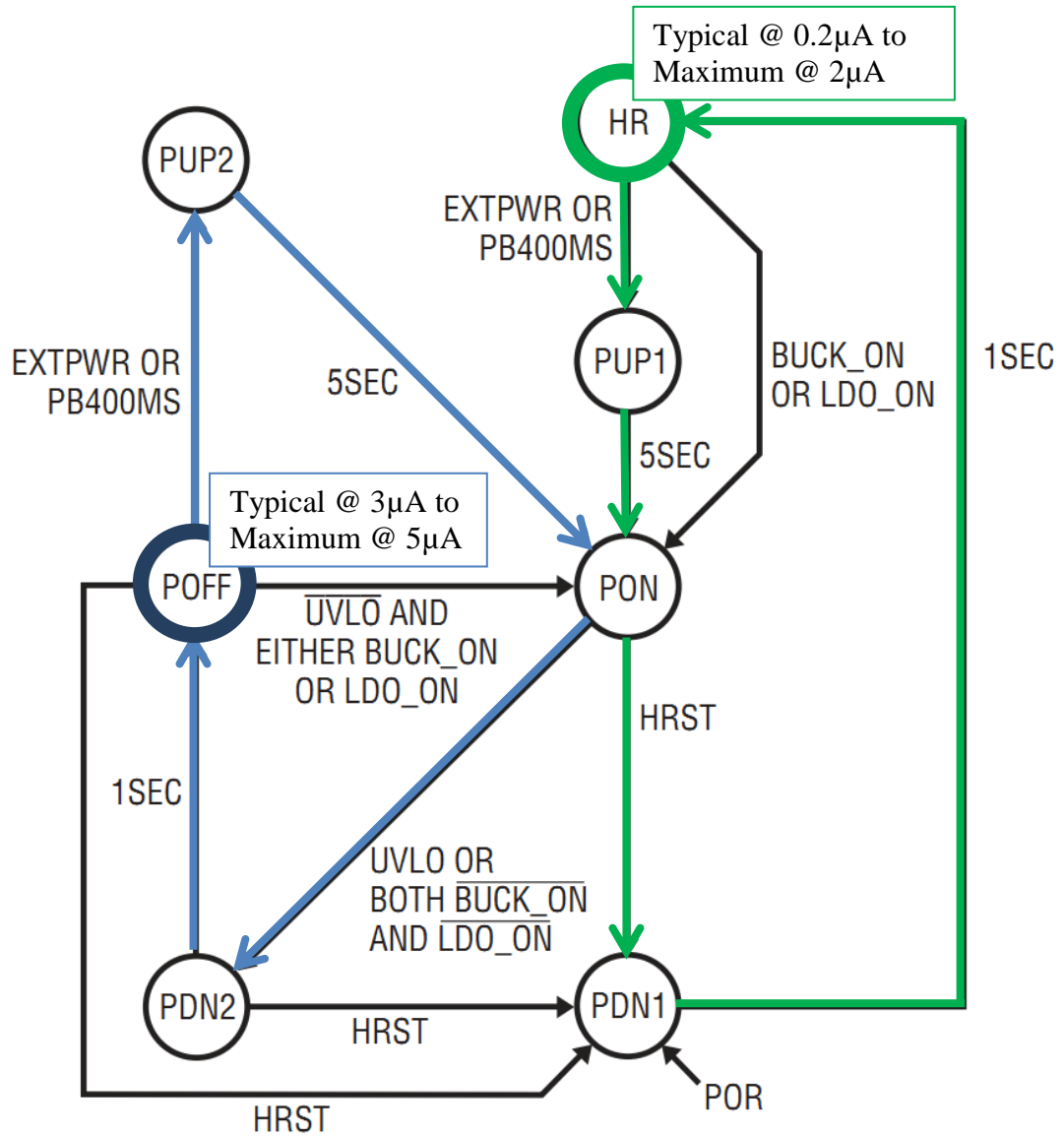
**Figure 38: Pushbutton state diagram** [37]

The LTC3553 also support Li-Ion battery charging via the USB port. The battery on the ECG device should be charged within 2 hours based on requirement R.O.5.1. With regards to the USB 2.0 specifications, a unit load is defined as 100mA. The USB 2.0 Specifications allow a maximum unit load of 5 which is equivalent to 500mA [49]. Equation $6-12$ specifies the formula for LTC3553 Li-Ion Charger charge current where $R_{PROG}$ resistance is valued at 3kΩ as shown in Equation $6-13$ [37].

$$I_{CHG}(A) = \frac{750V}{R_{PROG}} \qquad (6-12)$$

$$R_{PROG} = 3k\Omega \qquad\qquad (6-13)$$

$$I_{CHG}(A) = 250mA \qquad\qquad (6-14)$$

$I_{CHG}$ is found to be at 250mA as shown in Equation $6-14$. Theoretically, this means that a full charge on a battery capacity of 420mAh requires about 1hour 41minutes. Note that the $R_{PROG}$ can be varied to adjust the $I_{CHG}$ current up to 500mA as supported by the USB 2.0 specifications. If 500mA were to be the desired current charge, $R_{PROG}$ should be changed to $1.5k\Omega$ [37]

## 6.3    Results and Comparisons

The setup methodology is first defined for both the CB ECG and BLE ECG device. This is followed by the validation of AFE used against commercial ECG device. The battery discharge plot between various ECG devices and configuration will be presented. This is then followed by the overall system verification and validation to the requirements specifications.

### 6.3.1   Setup Methodology

With the ECG device in place, the setup methodology to capture the ECG data is described. Figure 39 illustrates the placement of the electrodes on a skeletal diagram and on an actual candidate. Lead I* is taken from B-C, Lead II* is taken from A-C and Lead III* is taken from A-B. Note that 'R' is the reference electrode or ground. In this configuration, Lead II is used as both ECG and impedance measurement yielding heart rate and respiratory rate respectively. The electrodes that are not labeled belong to Welch Allyn

(Commercial ECG device) and the electrode placement is done on a standard 12-lead ECG as discussed in Section 2.1.1. Measurements from both the Welch Allen ECG device and the target ECG device are taken simultaneously for 5 minutes. In addition, the Li-Ion battery of 420mAh is used to power up the ECG device.
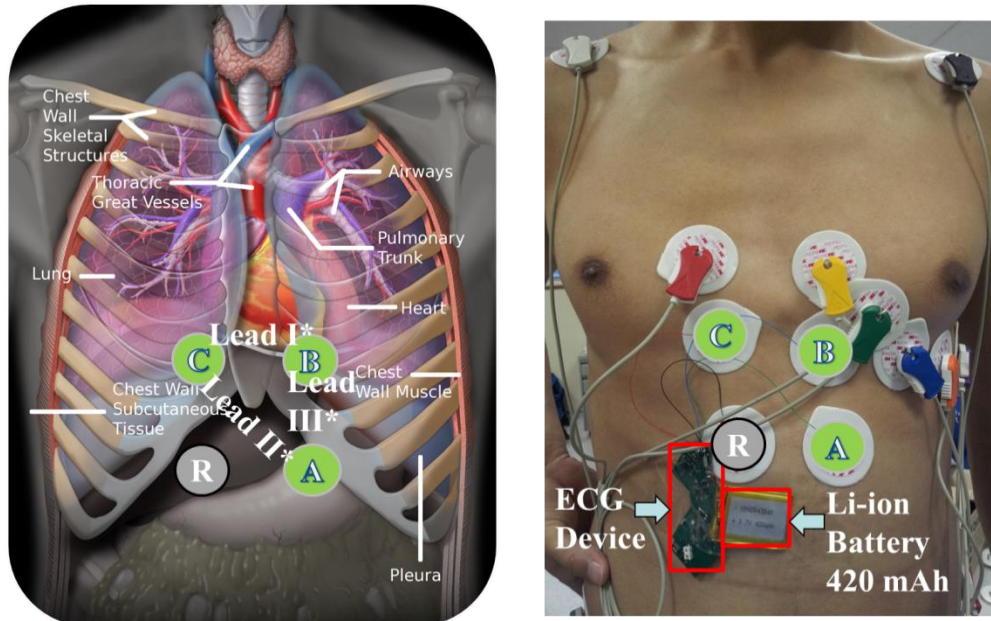


**Figure 39: ECG and electrodes on trial**

## 6.3.2 Accuracy of ECG AFE

In this subsection, lead to lead comparison plots and histograms are made on Matlab to verify the accuracy. The single-lead NUS ECG Chip with buffer mode has been verified in [5] .The 2-channel NUS ECG Chip with Compression [27] (compression deactivated) is compared against the commercial Welch Allyn for accuracy. From this point onwards, NUS Chip synonymous to NUS ECG Chip with Compression.

Figure 40 illustrates a lead to lead comparison between NUS Chip and Welch Allyn. The default sampling rate of the NUS Chip and Welch Allyn

device are 256Hz and 600Hz respectively. The first, second, third and fourth

plots in Figure 40 are NUS Chip Lead I*, NUS Chip Lead II* and NUS Chip

Lead III* and Welch Allyn Lead II. The 2-channel ECG chip yields Lead I*

and Lead III* and Lead II* is derived by the sum of Lead I* and Lead III*.

The lead to lead comparison in Figure 40 is plotted against time for about 20

seconds. Note that the Welch Allyn ECG has been down sampled from 600Hz

to 256Hz for consistency during comparison. The down sampling is done by

using the resample() command in Matlab.
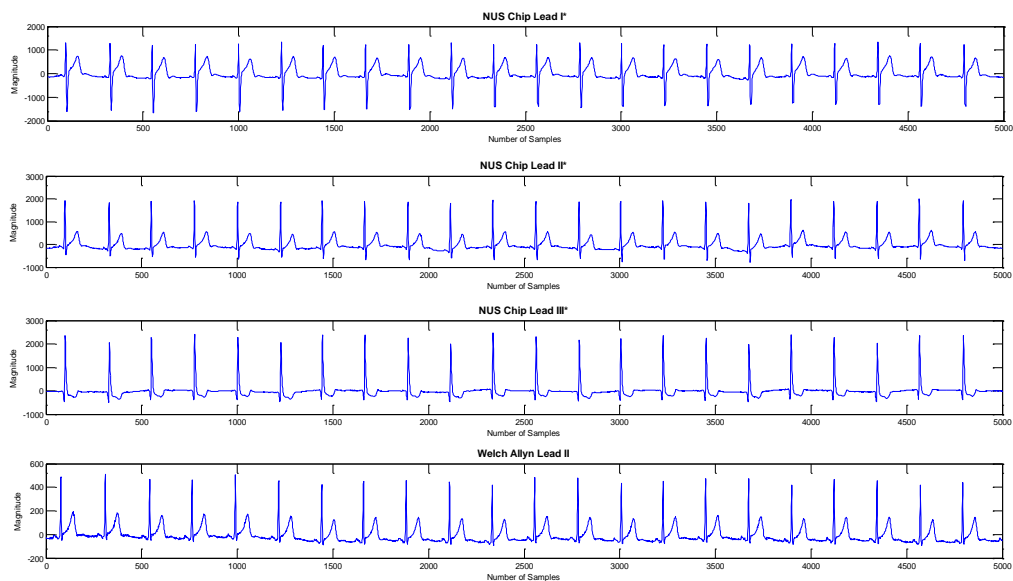


**Figure 40: NUS Chip vs Welch Allyn**

Figure 41 illustrates the histogram on the RR interval for the Welch Allyn

ECG device (top) and NUS chip (bottom). The RR interval from the Lead II of

Welch Allyn is compared against the RR interval from the Lead II* of NUS

chip. The shape of both the histogram is visually quite similar. In order to

establish equality, it is also noted that the peak or mode occurred at 800ms for

both Welch Allyn Device and NUS Chip.
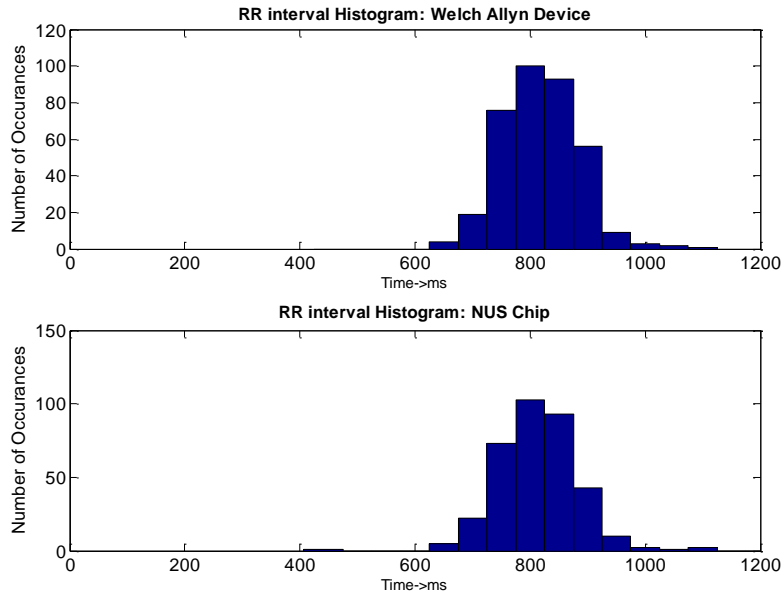
**Figure 41: Histogram on RR for Welch Allyn (top) vs NUS chip (bottom)**

Figure 42 illustrates a lead to lead comparison between TI ADS1292R Chip (Lead II – row 2) and Welch Allyn (Lead II – row 3) along with a bio-impedance plot (row 1). The ADS1292R supports 2 channels ECG or single channel ECG cum single bio-impedance measurement. The $2^{nd}$ option is selected. This means that the device will provide a single-lead ECG along with a single bio-impedance. The respiratory rate can be derived from the bio-impedance waveform.

The default sampling rate of the ADS1292R and Welch Allyn device are 250Hz and 600Hz respectively. The lead to lead comparison (row 2 and row 3) in Figure 42 is plotted against time of about 20 seconds. Note that the Welch Allyn ECG has been down sampled from 600Hz to 250Hz for consistency during comparison. The down sampling is done by using the resample() command in Matlab. From Figure 42, the impedance strip (row 1)

shows that there are about 7 breaths (7 humps) in 20 seconds which is

evaluated as 21 breaths per minute.



**Figure 42: ADS1292R vs Welch Allyn**
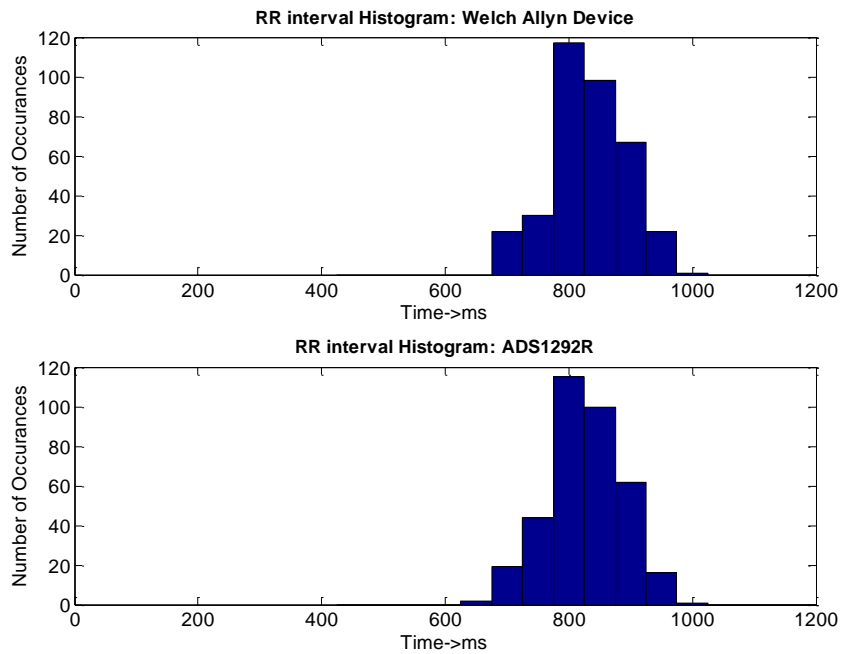


**Figure 43: Histogram on RR for Welch Allyn (top) vs ADS1292R (bottom)**

Figure 43 illustrates the histogram on the RR interval for the Welch Allyn

ECG device (top) and the Texas Instruments ADS1292R chip (bottom). The

RR interval from the Lead II of Welch Allyn is compared against the RR

interval from the Lead II* of ADS1292R. The shape of both the histogram is visually quite similar. In order to establish equality, it is also noted that the peak or mode occurred at 800ms for both Welch Allyn device and ADS1292R chip.
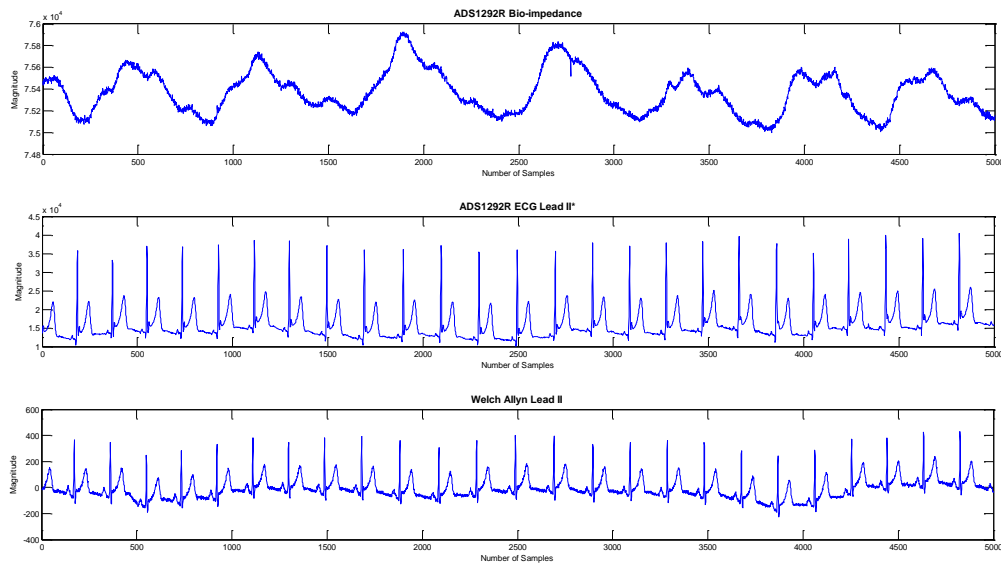
**Table 15 Average RR Difference between Welch Allyn, NUS Chip and ADS1292**

| ECG Chip | Welch Allyn | NUS Chip | ADS1292R |
|---|---|---|---|
| *Sampling Rate* | 600Hz | 256Hz | 250Hz |
| *Average Heart Rate* | 75BPM | 75BPM | 75BPM |

Table 15 shows the comparative results between Welch Allyn, NUS chip and ADS1292R chip. As shown, the Welch Allyn, NUS chip and ADS192R have the same average heart rate when compared against the commercial Welch Allyn.

### 6.3.3 Battery Discharge Plot

The Li-Ion battery profiling on various in-house devices and configurations during continuous transmission is shown in Figure 44. There are 2 devices (CB ECG device and BLE ECG device) running on a full charged 420mAh Li-Ion battery at an ECG sampling rate of about 250Hz to 256Hz. The variation is because NUS ECG chips support 256Hz and the ADS1292R supports 250Hz. It can be seen that the CB ECG device on Classic Bluetooth (red) has the shortest battery life span of about 13 hours and 20 minutes with an average current consumption of 31.5mA.
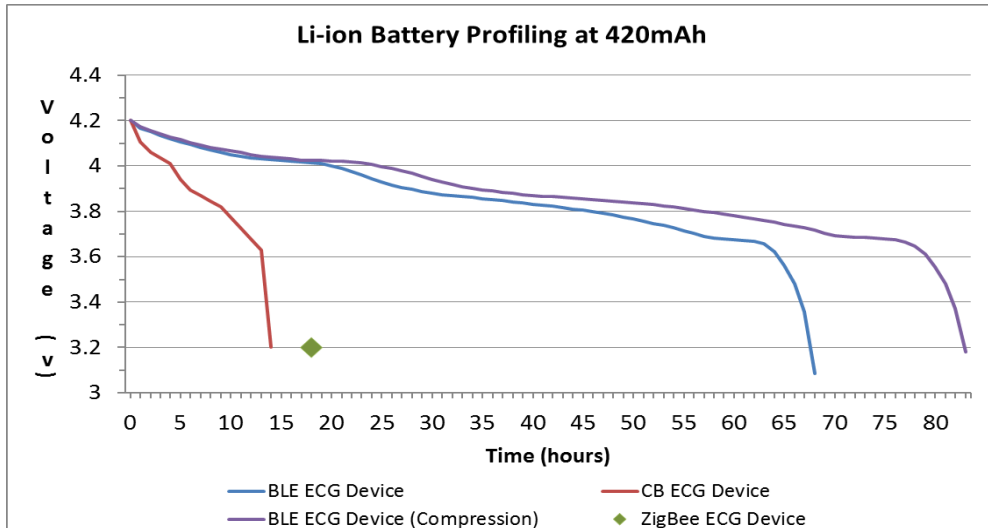
**Figure 44: Profiling battery discharge for continuous transmission**

The results of a single-lead ZigBee ECG device on CC2420 (green) is referenced from [13]. It has a Li-Ion capacity of 620mAh (26 hours) which is normalised to 420mAh (~18 hours). The low-power BLE ECG device on CC2540 (blue) has made significant improvement allowing battery life of about 68 hours. The improvement is much attributed to the integrated SoC (MCU and transceiver) and power improvements in BLE technology. When the lossless compression algorithm (Section 6.2.2) is implemented, the current drawn from the BLE ECG device (purple) dropped to about 5mA enabling about 83 hours of continuous operation. This improvement is about 6.5 times from the reference commercial wireless ECG device, Spyder. Note that each line (red, blue and purple) has a gradual discharge pattern. When the voltage reaches about 3.7V, the gradient decent becomes steeper owing to the properties of Li-Ion battery discharging characteristics. The details of the battery discharge plot (Figure 44) and commercial ECG, Spyder, are tabulated on Table 16. It shows that the low-power BLE ECG device (2.83 days without compression and 3.46 days with compression) can achieve power reduction of up to 5 times as compared to the commercial wireless ECG device.

Table 16: Results of 420mA battery profiling on various profiles of ECG devices

| Assuming ECG Device on 420mAh Battery Regulated at 3.3V | Power | Duration | Improvements |
|---|---|---|---|
| Spyder | 109.89mW @ 33.3mA | ~ 12 hours 30mins | *[Reference]* |
| CB ECG Device | 103.95mW @ 31.5mA | ~13 hours 20mins | 1.06x |
| ZigBee ECG Device | 78.71mW @ 23.9mA | ~17hours 40mins | 1.40x |
| BLE ECG Device | 20.39mW @ 6.18mA | ~68 hours (2.83 days) | 5.39x |
| BLE ECG Device (Compression) | 16.70mW @ 5.06mA | ~83 hours (3.46 days) | 6.58x |

## 6.3.4 Overall System Verification and Validation

Verification and validation is defined as "the process of determining whether the requirements for a system or component are complete and correct, the products of each development phase fulfill the requirements or conditions imposed by the previous phase, and the final system or component complies with specified requirements" [50] [51]. Table 17 tabulates the user requirements to the design and implementation of the ECG device with reference to the low-power BLE ECG device of Section 6.2. The row 'O/M' means optional or mandatory requirements. It is noted that all requirements have been achieved.

Table 17: Checklist of requirements to design and implementation with regards to the low-power BLE ECG device

| Requirements | Design and Results | O/M | Achieved? |
|---|---|---|---|
| **R.M.1. Display and Ensuring Accuracy of ECG AFE** | | | |
| R.M.1.1. The ECG device must be able to stream at least 1-lead ECG signal to a | The real-time ECG signal is display on the smartphone of the client | M | *Yes* |

| | | | |
|---|---|---|---|
| smartphone in real-time. | application in Section 5.2.6. | | |
| R.M.1.2. The ECG sensor must be of resolution of at least 12 bits. | All ECG sensors described in Section 4.2 supports at least 12-bits. | M | *Yes* |
| R.M.1.3. The sampling rate of the ECG sensor must be least 250Hz. | All ECG sensors described in Section 4.2 are configured to support at least 250Hz. | M | *Yes* |
| R.M.1.4. The heart rate derived from the waveform produced by the low-power wireless ECG device must be comparable to a commercial ECG device. | Section 6.3.2 shows that the heart rate obtained for Welch Allyn (commercial) against NUS chips and TI ADS1292R are similar. | M | *Yes* |
| **R.M.2. ECG Lead Status Detection** | | | |
| R.M.2.1. ECG chip should be able to detect lead-off. | All ECG chips described in Section 4.2 and used in Section 6.1 and 6.2 have the lead-off detection feature. | M | *Yes* |
| R.M.2.2. The ECG device should alert the user during lead-off via the client application. | The client application supports lead-off alerts as shown in Section 5.2.4 and Section 5.2.6. | M | *Yes* |
| R.M.2.3. ECG device's LED toggles during lead-off. | During Standby and Transmit Data state, the state machine in Section 5.1.2 will toggle the LED when lead-off happens. | M | *Yes* |
| R.M.2.4. ECG device's LED is solid during lead-on. | During Standby state, the LED will turn solid when lead-on happens as shown in Section 5.1.2. | M | *Yes* |
| R.M.2.5. In addition to R.M.2.4, during ECG transmission, ECG device's LED will glow. | During Transmit Data state, the LED will glow solid when lead-on happens as shown in Section 5.1.2. | M | *Yes* |
| **R.M.3. Event Marker During ECG Monitoring.** | | | |
| R.M.3.1. Button on the ECG device to indicate an event marker during the ECG monitoring. | This feature is supported by the state machine in the 'Transmit Data' state as shown in Section 5.1.2. The event marker is demonstrated on the smartphone in Section 5.2.6. Section 6.1 and | M | *Yes* |

| | Section 6.2 shows that there is a button connected on the block diagrams. | | |
|---|---|---|---|
| **R.M.4. Wireless Transmission Between Smartphone and ECG device.** | | | |
| R.M.4.1. The communication between the sensor and the personal gateway (smartphone) should be done via the wireless medium. | The smartphone uses the Bluetooth interface to communicate with the ECG sensor as shown in Section 5.2.6. The block diagrams of Section 6.1 and Section 6.2 have the block containing the Bluetooth interface. | M | *Yes* |
| **R.M.5. Low-power During Continuous ECG Transmission.** | | | |
| R.M.5.1. At least 3 times the power reduction as compared to the commercial wireless ECG device, Spyder. | The lossless compression algorithm has been implemented in the SoC embedded with a low power transceiver as shown in Section 6.2.2. The results of the power reduction can be seen in Section 6.3.3. | M | *Yes* |
| **R.M.6. Rechargeable Battery.** | | | |
| R.M.6.1 The ECG device should be powered up by a rechargeable Li-Ion battery of 420mA. | The Li-Ion battery is used as shown in Figure 39 of Section 6.3.1. | M | *Yes* |
| R.M.6.2 The rechargeable battery can be recharged when not in use. | The state machine in Section 5.1.2 facilitates a Charging state. A hardware fast charge configuration on LTC3553 is described in Section 6.2.3. | M | *Yes* |
| **R.M.7. Low on the Shelf Battery Discharge** | | | |
| R.M.7.1 The battery drain when the device is not operational (sleep mode) should not go beyond 15μA. | The technique for minimal battery leakage is supported by the LTC3553 IC and is described in Section 6.2.3. This method is similar to the power gating techniques by un-powering the voltage rails of the voltage regulator. | M | *Yes* |
| **R.O.1. Heart Rate Indicator** | | | |

| | | | |
|---|---|---|---|
| R.O.1.1. The heart rate should be displayed on the client application. | The heart rate is display on the PC application and smartphone as shown in Section 5.2.5 and Section 5.2.6 respectively. | O | *Yes* |
| R.O.1.2. The heart rate can be calculated from the ECG waveform via two successive RR peaks. | The ECG to heart rate signal processing is described in Section 5.2.3. | O | *Yes* |
| **R.O.2. Display Battery Life of the ECG device** | | | |
| R.O.2.1 ECG device should support power monitoring. | The SoC of the low-power BLE ECG device has ADC capabilities as tabulated in Table 11. Figure 31 also shows pin P0_7 and P1_0 in supporting the battery monitoring feature. | O | *Yes* |
| R.O.2.2 Display the battery life on the client application. | The client application shows the battery life as shown in Figure 25 and Figure 26 of Section 5.2.5 and Section 5.2.6 respectively. | O | *Yes* |
| **R.O.3. Measure The Activity Of The End-user** | | | |
| R.O.3.1 To measure how active the user has been when the device is worn by the user. | The BLE ECG device's PCB has an accelerometer as shown in Figure 30. The proper acceleration from the accelerometer is converted into activity index as explained in Section 5.2.2. The client application indicates the activity index as shown in Figure 25 and Figure 26 of Section 5.2.5 and Section 5.2.6 respectively. | O | *Yes* |
| **R.O.4. Ambient Temperature** | | | |
| R.O.4.1 The ambient temperature is measured when the device is worn by the user. | The client application on the PC and smartphone as shown in Section 5.2.5 and Section 5.2.6 can display the ambient temperature. This is possible with the support of the state machine as defined in Section 5.1.2. | O | *Yes* |

| R.O.5. Fast Charge Of Less Than 2 Hours | | | |
|---|---|---|---|
| R.O.5.1 The charge time of the rechargeable battery should not exceed 2 hours. | With the LTC3553 and configurations as shown in Section 6.2.3, a full charge will take less than 2 hours (1hour and 41minutes) | O | *Yes* |
| **R.O.6. Respiratory Rate** | | | |
| R.O.6.1 Measure the respiratory rate when the device is worn by the user. | The ADS1292R support bio-impedance measurement and results are plotted in Figure 42. The respiratory rate can be derived from the waveform. | O | *Yes* |
| **R.O.7. Storing the ECG Samples** | | | |
| R.O.7.1 The ECG samples can be stored in the ECG device or on the smartphone. | The client application on the smartphone as shown in Section 5.2.6 is able to store the ECG data. | O | *Yes* |

## 6.4    Conclusion

The hardware software co-design techniques were applied on the CB ECG device and the BLE ECG device. These techniques include the selection of the integrated SoC, lossless ECG compression, usage of a power management unit to reduce dynamic and static power dissipation, etc. The low-power BLE ECG device can support about 3 days of continuous transmission on a 420mAh battery. Finally, the verification and validation was made to crosscheck between the requirements and design.

# 7    Conclusion and Future Works

This work has presented the requirements, design and implementation of a low-power wireless ECG device aimed at continuous wearable cardiac monitoring. The thesis highlights two types of ECG devices, a Classic Bluetooth ECG (CB ECG), and a low-power Bluetooth Low Energy (BLE) ECG device. The Classic Bluetooth (Bluetooth 2.1 EDR) device can be used for multi-lead transmission (capable of supporting up to 12-lead ECG) whereas BLE device is suitable for continuous streaming on a limited number of channels. The Bluetooth standard is chosen as the interface for inter-device communication between the ECG device and smartphone because of its availability and maturity. In addition, Bluetooth consumes lesser power compared to other communication standards.

For designing the low-power embedded wireless ECG device, several techniques such as voltage scaling, frequency scaling, toggling between active/idle mode and low leakage power management were applied. The design also focused on optimal hardware software co-design methodologies for the use of low-complexity lossless gradient based compression algorithm. A power discharge plot, while on continuous data transmission with a fully charged 420mAh battery was recorded on various ECG hardware platforms. It shows that BLE ECG (20.39mW @ 6.18mA) on the CC2540 SoC is suitable for single-lead transmission because the power drawn in comparison to CB ECG device (103.95mW @ 31.5mA) is substantially lower. The continuous ECG data transmission on the low-power BLE ECG device can last for about 68 hours. The battery life of the BLE ECG device extends for another 15

hours after the addition of the low-complexity lossless compression algorithm. This highlights the importance of selecting the target hardware (fine-grained CC2540 with BLE) that can leverage the compression algorithm for further power reduction, in contrast to the Classic Bluetooth module. The accuracy of the ECG sensors within the ECG device has been established to ensure data integrity. The NUS ECG chip was benchmarked against a commercial ECG device. Overall system verification and validation for the low-power BLE ECG device shows that all the 7 mandatory and 7 optional requirements were achieved.

For future works, the work done in this thesis can serve as a reference design or platform to test new compression algorithm. Future works may also include using a more efficient SoC such as the CC2541. On-chip hardware compression can be implemented along with CC2541 SoC for further power reduction during continuous data transmission as compared to firmware implementations. The dual-stack (Classic Bluetooth and BLE) bridge mode on CC2564 can be coupled together with a low-power MCU MSP430FRAM [52] for a smart power-aware wireless ECG device that can scale between a low-throughput and high-throughput transmission.

# Bibliography

[1]     S. Chronic and U. States, *Vital and Health Statistics Selected Chronic Conditions : Conditions :*, 10th ed., no. 194. National Center for Health Statistics USA, 1997, pp. 1 – 98.

[2]     A. S. Go, E. M. Hylek, K. A. Phillips, Y. Chang, L. E. Henault, J. V Selby, and D. E. Singer, "Prevalence of diagnosed atrial fibrillation in adults: national implications for rhythm management and stroke prevention: the AnTicoagulation and Risk Factors in Atrial Fibrillation (ATRIA) Study.," *JAMA*, vol. 285, no. 18, pp. 2370–5, May 2001.

[3]     A. Schuchert, R. Maas, C. Kretzschmar, G. Behrens, I. Kratzmann, and T. Meinertz, "Diagnostic yield of external electrocardiographic loop recorders in patients with recurrent syncope and negative tilt table test.," *Pacing Clin. Electrophysiol.*, vol. 26, no. 9, pp. 1837–40, Sep. 2003.

[4]     M. Tsai, "Inside DSP on Low Power: Designing Low-Power Signal Processing Systems," *EETimes: Design How-To*, 2004. [Online]. Available: http://www.eetimes.com/document.asp?doc_id=1272612. [Accessed: 17-Jan-2014].

[5]     D. R. Zhang, "Design Of Energy Efficient Wearable ECG System And Low Power Asynchronous Microcontroler," National University of Singapore, 2012.

[6]     D. L. T. Wong and Y. Lian, "A wearable wireless ECG sensor with real-time QRS detection for continuous cardiac monitoring," in *2012 IEEE Biomedical Circuits and Systems Conference (BioCAS)*, 2012, pp. 112–115.

[7]     E. Z. Gorodeski, H. Ishwaran, U. B. Kogalur, E. H. Blackstone, E. Hsich, Z. Zhang, M. Z. Vitolins, J. E. Manson, J. D. Curb, L. W. Martin, R. J. Prineas, and M. S. Lauer, "Use of hundreds of electrocardiographic biomarkers for prediction of mortality in postmenopausal women: the Women's Health Initiative.," *Circ. Cardiovasc. Qual. Outcomes*, vol. 4, no. 5, pp. 521–32, Sep. 2011.

[8]     J. Gravning and J. Kjekshus, "The perfect biomarker in acute coronary syndrome: a challenge for diagnosis, prognosis, and treatment.," *Eur. Heart J.*, vol. 29, no. 23, pp. 2827–8, Dec. 2008.

[9]     J. Malmivuo and R. Plonsey, *Bioelectromagnetism: principles and applications of bioelectric and biomagnetic fields*. New York: Oxford University Press, 1995.

[10] B. M. D. Wilburta Q. Lindh, Marilyn S. Pooler, Carol D. Tamparo, *Comprehensive Medical Assisting Administrative and Clinical Competencies.: Administrative and Clinical Competencies*, 4th ed. Cengage Learning, pp. 573 – 1.

[11] R. F. Yazicioglu, S. Kim, T. Torfs, H. Kim, and C. Van Hoof, "A 30 uW Analog Signal Processor ASIC for Portable Biopotential Signal Monitoring," *Solid-State Circuits, IEEE Journal of*, vol. 46, no. 1. pp. 209–223, 2011.

[12] J. A. G. Gnecchi, F. O. Vargas, V. H. O. Peregrino, and D. L. Espinoza, "Design and Construction of a Continuous Ambulatory Electrocardiogram Recorder, Auxiliary in the Detection of Cardiac Arrhythmias," *2010 IEEE Electron. Robot. Automot. Mech. Conf.*, pp. 602–606, Sep. 2010.

[13] D. R. Zhang, C. J. Deepu, X. Y. Xu, and Y. Lian, "A wireless ecg plaster for real-time cardiac health monitoring in body sensor networks," *Biomed. Circuits Syst. Conf. (BioCAS), 2011 IEEE*, pp. 205–208, 2011.

[14] "AliveCor ® Heart Monitor User Manual," p. 16, 2013.

[15] "Spyder Bluetooth User Manual SPBT20A," Singapore, 2012.

[16] P. Arun and S. Ramasamy, "A low-power dual threshold voltage-voltage scaling technique for domino logic circuits," *Computing Communication & Networking Technologies (ICCCNT), 2012 Third International Conference on*. pp. 1–6, 2012.

[17] J. M. Rabaey, A. Chandrakasan, and B. Nikolic, *Digital Integrated Circuits*, 2nd ed. Prentice Hall, 2003, pp. 213–10.

[18] P. Ehrlich and S. Radke, "Energy-aware software development for embedded systems in HW/SW co-design," *Design and Diagnostics of Electronic Circuits & Systems (DDECS), 2013 IEEE 16th International Symposium on*. pp. 232–235, 2013.

[19] F. Balarin, M. Chiodo, and A. Ferrari, "A Framework for Hardware-Software Co-Design of Embedded Systems," 2014. [Online]. Available: http://embedded.eecs.berkeley.edu/Research/hsc/abstract.html. [Accessed: 04-Jan-2014].

[20] "Wi-Fi Selector Guide," p. 1.

[21] "Wireless Module 802.11abgn, Wide Temperature WYSBMVGX1-I & WBSBMWGX4-I Overview," 2013.

[22] "Bluetooth 4.0 - Architecture & Terminology Overview," vol. 1, no. June, 2010.

[23] "Bluetooth 4.1 - Architecture & Terminology Overview," vol. 1, no. December, 2013.

[24] "Bluetooth 2.1 EDR - Architecture & Terminology Overview," vol. 1, no. July, 2007.

[25] Bluetooth Special Interest Group (SIG), "BLUETOOTH LOW ENERGY REGULATORY ASPECTS," vol. 10r00, no. April, pp. 1–30, 2011.

[26] S.-L. Chen and J.-G. Wang, "VLSI implementation of low-power cost-efficient lossless ECG encoder design for wireless healthcare monitoring application," *Electron. Lett.*, vol. 49, no. 2, pp. 91–93, Jan. 2013.

[27] C. J. Deepu, X. Zhang, W.-S. Liew, D. L. T. Wong, and Y. Lian, "An ECG-SoC with 535nW / Channel Lossless Data Compression for Wearable Sensors," *2013 IEEE Asian Solid-State Circuits Conf.*, pp. 145–148, Nov. 2013.

[28] J. R. Cox, F. M. Nolle, H. A. Fozzard, and G. C. Oliver, "AZTEC, a Preprocessing Program for Real-Time ECG Rhythm Analysis," *Biomedical Engineering, IEEE Transactions on*, vol. BME-15, no. 2. pp. 128–129, 1968.

[29] L. W. Gardenshire, *Data Redundancy Reduction For Biomedical Telemetry*, Biomedical., no. New York Academic Press. San Diego: Academic Press, 1965, pp. 255 – 298.

[30] S. M. Jalaleddine, C. G. Hutchens, R. D. Strattan, and W. a Coberly, "ECG data compression techniques--a unified approach.," *Biomed. Eng. IEEE Trans.*, vol. 37, no. 4, pp. 329–43, Apr. 1990.

[31] T. Blanchett, G. C. Kember, and G. A. Fenton, "KLT-based quality controlled compression of single-lead ECG," *Biomedical Engineering, IEEE Transactions on*, vol. 45, no. 7. pp. 942–945, 1998.

[32] L. V Batista, L. C. Carvalho, and E. U. K. Melcher, "Compression of ECG signals based on optimum quantization of discrete cosine transform coefficients and Golomb-Rice coding," *Engineering in Medicine and Biology Society, 2003. Proceedings of the 25th Annual International Conference of the IEEE*, vol. 3. pp. 2647–2650 Vol.3, 2003.

[33] U. E. Ruttimann and H. V Pipberger, "Compression of the ECG by Prediction or Interpolation and Entropy Encoding," *Biomedical Engineering, IEEE Transactions on*, vol. BME-26, no. 11. pp. 613–623, 1979.

[34] G. Nave and A. Cohen, "ECG compression using long-term prediction," *Biomedical Engineering, IEEE Transactions on*, vol. 40, no. 9. pp. 877–885, 1993.

[35] A. Koski, "Lossless ECG Encoding," *Comput. Methods Progr. Biomed.*, vol. 52, no. 1.

[36] Z. Arnavut, "ECG Signal Compression Based on Burrows-Wheeler Transformation and Inversion Ranks of Linear Prediction," *Biomedical Engineering, IEEE Transactions on*, vol. 54, no. 3. pp. 410–418, 2007.

[37] L. Dropout and L. D. O. Linear, "LTC3553 - Micropower USB Power Manager With Li-Ion Charger, LDO and Buck Regulator," pp. 1–36.

[38] "ADS1292R Low-Power , 2-Channel , 24-Bit Analog Front-End for Biopotential Measurements ADS1291 ADS1292R," 2012.

[39] "WT12 Datasheet," *Bluegiga*, no. November, pp. 1–52, Nov-2013.

[40] "KC-22 Class 2 Bluetooth Data Micro Module," *KC Wirefree*, pp. 1–13, Feb-2012.

[41] "Xtrinsic MMA8452Q 3-Axis, 12-bit/8-bit Digital Accelerometer," *Freescale Semiconductor*, pp. 1–47, Oct-2013.

[42] "PIC18F46J50 Family Data Sheet," *Microchip*, pp. 1–554, 2009.

[43] "2.4-GHz Bluetooth ® low energy System-on-Chip," *Texas Instruments*, no. June, pp. 1–35, Oct-2013.

[44] Bluetooth Special Interest Group (SIG), "BLUETOOTH SPECIFICATION Version 4.1," vol. 0, 2013.

[45] E. White, *Making Embedded Systems: Design Patterns for Great Software*. O'Reilly Media, 2011, pp. 1 – 330.

[46] B. P. Douglass, *Real-Time Design Patterns: Robust Scalable Architecture for Real-Time Systems*. Addison-Wesley Professional, 2002, pp. 1–528.

[47] B. P. Douglass, *Design Patterns for Embedded Systems in C: An Embedded Software Engineering Toolkit*, 1st ed. Newnes, 2010, pp. 1 – 472.

[48] C. M. Gibson, S. P. Patel, K. Goel, and C. Zorkun, "EKG artifacts," *ECGpedia*, 2008. [Online]. Available: http://static.wikidoc.org/5/5e/BaselineDrift.png. [Accessed: 18-Jan-2014].

[49]  R. (Texas I. Kollman and J. (Texas I. Betten, "Powering electronics from the USB port," *Analog Appl. J.*, no. Power Management, pp. 28–35, 2002.

[50]  "IEEE Standard Glossary of Software Engineering Terminology," *IEEE Std 610.12-1990*. pp. 1–84, 1990.

[51]  I. Standard, "Systems and software engineering -- Vocabulary," *ISO/IEC/IEEE 24765:2010(E)*, vol. 2010, pp. 1–418, 2010.

[52]  M. Zwerg, A. Baumann, R. Kuhn, M. Arnold, R. Nerlich, M. Herzog, R. Ledwa, C. Sichert, V. Rzehak, P. Thanigai, and B. O. Eversmann, "An 82uA/MHz microcontroller with embedded FeRAM for energy-harvesting applications," *Solid-State Circuits Conf. Dig. Tech. Pap. (ISSCC), 2011 IEEE Int.*, vol. 4, no. 3, pp. 334–336, 2011.
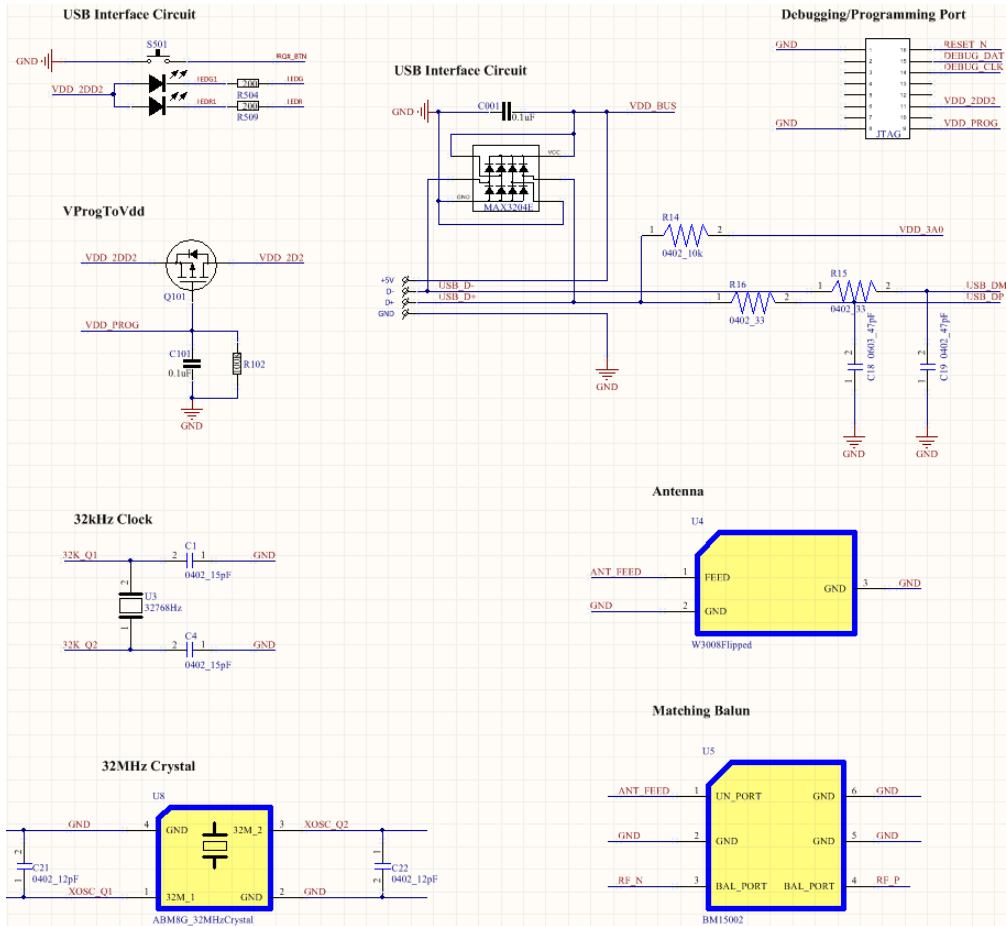
# Appendix A
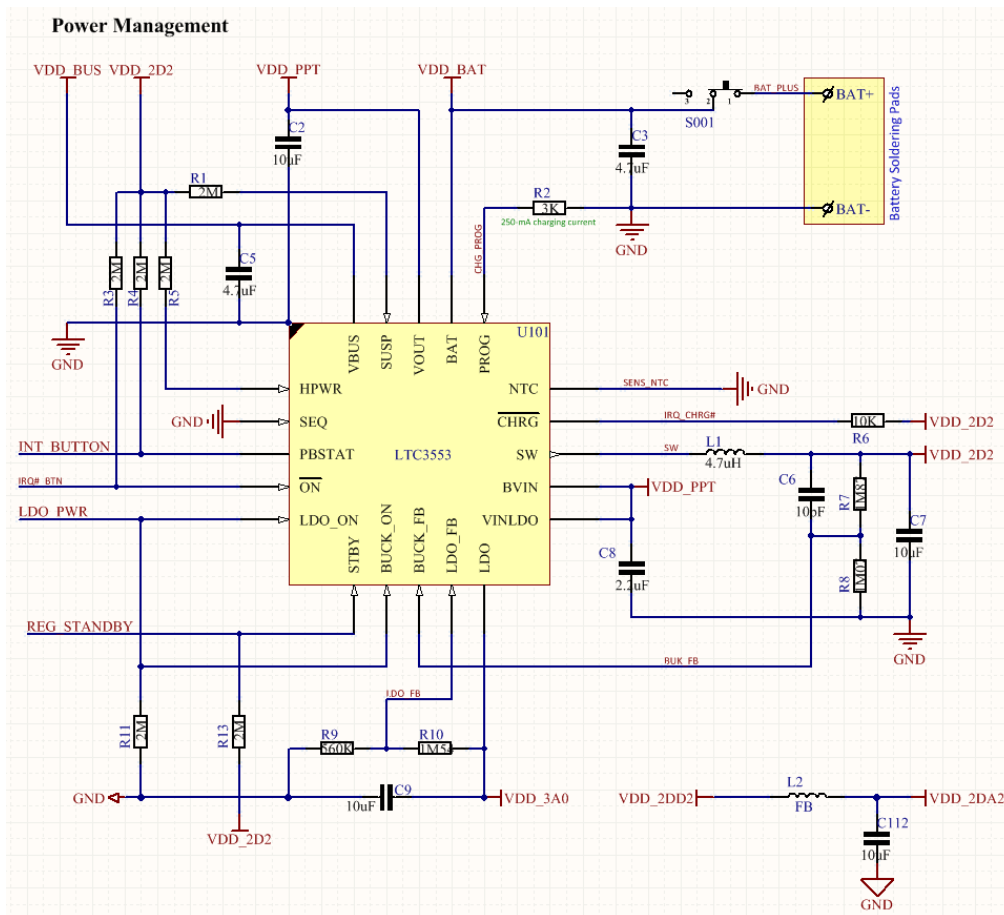


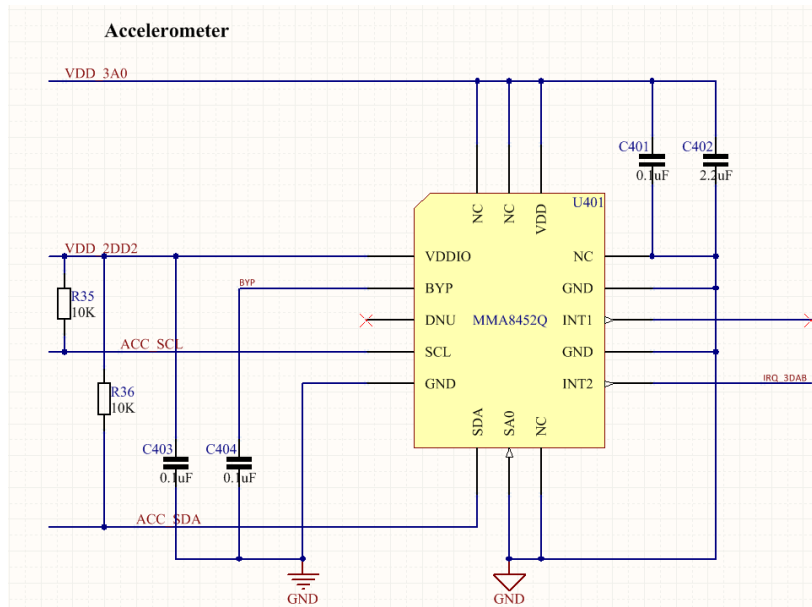**Power Management IC – LTC3553 by Linear Technology**
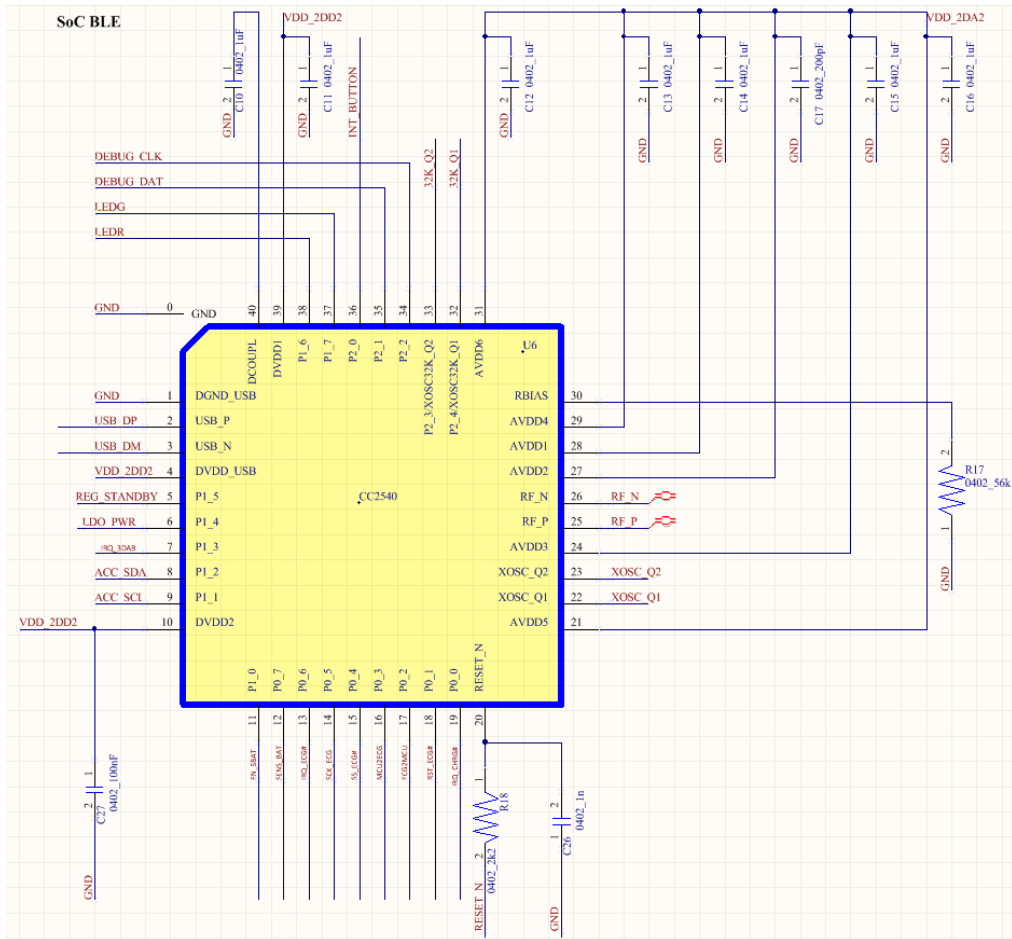
**BLE 4.0 SoC CC2540 by Texas Instruments**

**Various Component Interfaces of CC2540**


**3-Dimensional Accelerometer MMA8452Q by Freescale Seminconductor**

**AFE ECG and Bio-impedance ADS1292R by Texas Instruments**